EFFECT OF SOURCE INDUCTANCE ON SINGLE-PHASE FULLY CONTROLLED CONVERTER FED SEPARATELY EXCITED DC MOTOR

A Thesis Submitted
in Partial Fulfilment of the Requirements
for the Degree of

MASTER OF TECHNOLOGY

by

DILIP KUMAR CHAUBEY

to the

DEPARTMENT OF ELECTRICAL ENGINEERING
INDIAN INSTITUTE OF TECHNOLOGY KANPUR
APRIL, 1986

CERTIFICATE

It is certified that this work 'EFFECT OF SOURCE INDUCTANCE ON SINGLE-PHASE FULLY CONTROLLED CONVERTER FED SEPARATELY EXCITED DC MOTOR' by Dilip Kumar Chaubey has been carried out under our supervision and that this work has not been submitted elsewhere for a degree.

(S.R. Doradla)
Professor

(G.K. Dubey)
Professor

Department of Electrical Engineering
Indian Institute of Technology
Kanpur, India

ACKNOWLEDGEMENT

I express my deep gratitude to my guides Dr. S.R. Doradla and Dr. G.K. Dubey for introducing me to the problem and providing constant help, guidance and encouragement throughout the course of this thesis work.

I am indebted to Dr. L.P. Singh for his encouragement and assistance during the work. I am grateful to Mr. P.N. Sreedhar, Mr. H.K. Patel and my friends. I must particularly mention Mr. P.G. Poonacha, K.G. Shastri and V.P. Singh in this regard.

I thank the laboratory staff of Electrical Engineering Department, particularly Mr. O.P. Arora, J.A. Usmani, D.N. Joshi and M.L. Gupta for their help and cooperation during the work.

Lastly, I thank Mr. J.S. Rawat for typing and Mr. Verma of Civil Engg. Dept. for drafting the figures.

Dilip Kumar Chaubey

TABLE OF CONTENTS

LIST OF FIGURES

LIST OF SYMBOLS

E_m	-	Peak value of ac voltage
BEMF	-	Back emf
i_a	-	Instantaneous armature current
v_a		Instantaneous armature voltage
i_s		Instantaneous source current
v_s		Instantaneous source voltage
α		Firing angle, rad.
β		Extinction angle, rad.
μ		Overlap angle, rad.
γ		Instant at which the supply voltage equals the back emf, rad.
γ'		$\pi-\gamma$, rad.
L_a		Armature inductance, H
R_a		Armature resistance, Ω
L_s		Source inductance, H
R_s		Resistance of source inductance, Ω
I_{ave}		Average value of armature current, A
T_{ave}		Average value of torque, N-M
M		Back emf constant, volt/RPM
K		Torque constant, Volts/RPS
ω		Freq. of supply voltage, rad/sec.
ℓ		step length

ABSTRACT

In any power supply, finite amount of inductance is present due to the leakage inductance of rectifier transformer and possibly due to the distribution network. The finite source inductance in power supply affects the performance of a converter fed separately excited dc motor because of the delay introduced in the commutation process. A study of the effect of source inductance on the performance of single-phase fully controlled converter fed separately excited dc motor has been presented in this thesis. Various modes of operation have been identified. A method for evaluating the performance of the dc motor is presented. The presence of source inductance reduces the area of discontinuous conduction but speed regulation becomes poor. The voltage harmonics, due to the delay in commutation process makes the power factor poor.

The theoretical results are compared with the experimental results. A good correlation has been found between the two. Oscillograms for certain modes have also been reported.

CHAPTER 1

INTRODUCTION

Since their invention in the late 19th century, the dc motors have been recognized as an ideal means of obtaining controlled rotational motion. The control of speed by variation of the armature voltage and field current makes the dc motor more flexible in operation. The dc motor can operate over a wide range of load conditions by the control of armature and field current.

The most flexible control is obtained by means of separately excited dc motor in which the armature and field current can be controlled independently. The speed control of a separately excited dc motor by a change in the field current is limited to the applications where constant power is satisfactory. The reduction in the field current, to increase the speed, reduces the torque. In addition it can not be changed quickly owing to the high inductance of the field winding. Hence, the field control is restricted to applications where constant power is desirable with variation in speed. The armature control in separately excited dc motor is independent of both the limitations since its field current is kept constant [1-3].

The speed control of dc motors is achieved by controlled rectification of ac supply by means of thyristor converters. Controlled rectification provides smooth variation of the speed both under motoring and regenerative braking. However, it produces ripple and discontinuous conduction in the armature current, harmonics in the source current and voltage. The presence of harmonics reduces the power factor. The presence of ripple increases the copper loss, reduces the commutation capability of the motor thus causes undesirable derating of the motor [4]. The discontinuous conduction makes the speed regulation poor. The discontinuous armature current depends on firing angle, load inductance, load resistance, and back emf.

The separately excited dc motor of low armature inductance and of medium rating, usually operates with discontinuous armature current when fed by a single-phase fully controlled converter. In case of discontinuous current operation, the output voltage waveform and hence its mean value is dependent upon the firing angle, armature inductance, resistance and back emf. Different types of output voltage waveforms are encountered depending upon the firing angle and armature circuit parameters. These are recognized here

as modes. The expression for voltage and current are different in different modes. Therefore, prior knowledge of these modes is desirable to evaluate the performance characteristics of the dc motor from the appropriate set of equations.

The detailed analysis of separately excited dc motor fed by a single-phase fully controlled converter under ideal supply conditions and various possible control methods have been presented in the references [5],[3]. In a realistic power supply, some amount of inductance will be present due to the leakage inductance of rectifier transformer and possibly due to the distribution network. The net inductance measured at the mains can be interpreted as internal inductance in the supply between the generator terminals and the mains. The source inductance or internal inductance of the supply introduces modes of discontinuous and continuous current operation which are different from the modes with zero source inductance. This is because of occurance of commutation process described in Section 3.1 of Chapter 3. The presence of source inductance adversally affects the performance of the dc motor and also of the supply system.

In this thesis, the analysis and performance of a separately excited $\int^{dc}$ motor fed by a single-phase fully controlled converter bridge with finite source inductance has been considered. The single-phase fully controlled converter fed by an ac source with finite source inductance gives reduced output voltage and introduces additional modes of operation due to finite time needed for the commutation of outgoing thyristors. All possible modes of operation, both for rectification and inversion have been described. The set of differential equations have been solved by numerical technique. Fourth order Runge-Kutta method has been used for the solution to evaluate performance of the drive. The theoretical results are verified by the experiments. The effect of source inductance on the drive performance has been evaluated.

This thesis is organized in five chapters. Chapter 1 is introduction. A brief review of available literature on the modes of operation and analysis of the system under considerations with and without source inductance, is presented in Chapter 2. Chapter 3 contains discription of modes, commutation process and the analysis. The differential equations describing different modes, have been solved

numerically by fourth order Runge-Kutta method to avoid lengthy expressions which are obtained by analytical solution. Flow-chart describing various steps used in the computer program has also been presented in Chapter 3.

Chapter 4 describes the experimental verification of the theoretical deductions. Different speed torque characteristics have been obtained experimentally for different values of source inductance. Continuous and discontinuous modes of conductions have been identified through experimental oscillograms. A comparision has been made between theoretical and experimental characteristics.

Chapter 5 presents the conclusion of the thesis. The motor ratings and parameters are given in Appendix I.

CHAPTER 2

LITERATURE-REVIEW

A brief review of the literature on the modes of operation and analysis of a single-phase fully controlled converter fed separately excited dc motor drive is presented in this chapter. The choice of extra inductance for continuous conduction in the armature circuit is discussed in Section 2.2.

2.1 SEPARATELY EXCITED DC MOTOR FED BY SINGLE-PHASE FULLY CONTROLLED CONVERTER WITH AN IDEAL SUPPLY:

The armature current of a separately excited dc motor fed by a single-phase fully controlled converter, shown in Fig. 2.1, is continuous or discontinuous depending on the firing angle, armature parameters and back emf. In the case of continuous armature current operation, the output voltage comprises only portions of ac supply voltage waveform. Therefore, the average value of this waveform is only dependent on the firing angles. As a result, the determination of the performance characteristics is simple. In the case of discontinuous armature current operation, the output voltage waveform depends on the firing angle, armature parameters and back emf. Hence, the analysis becomes slightly complex.

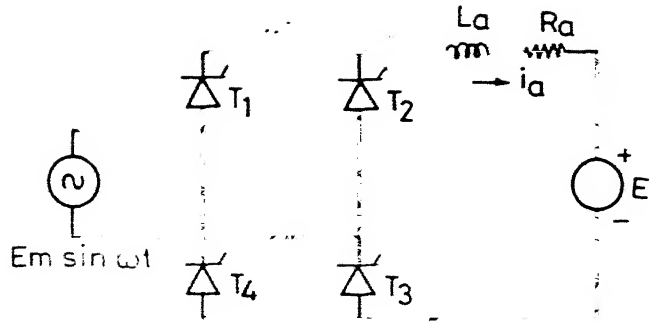

Fig. 2-1
Converter circuit

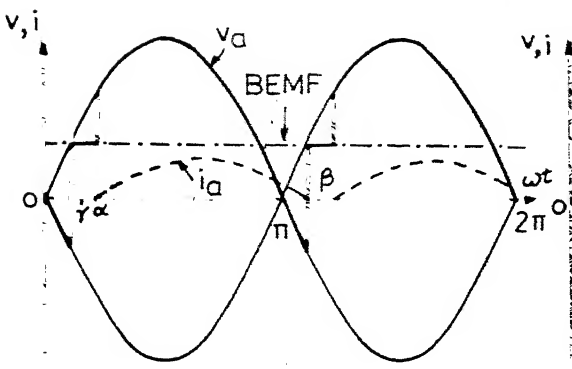

Fig. 2·2(a)

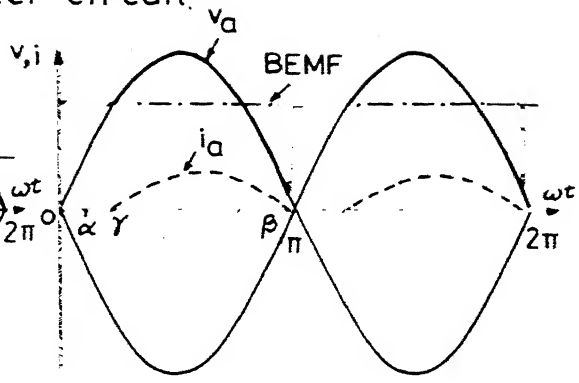

Fig. 2·2(b)

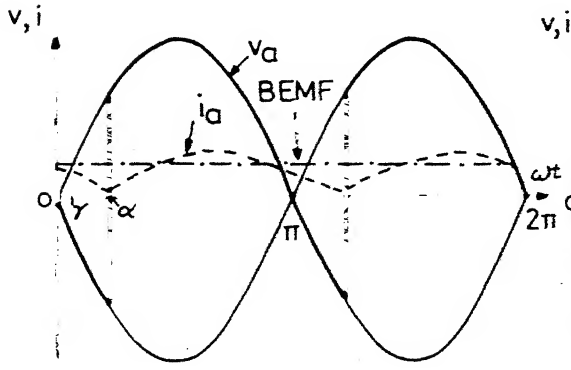

Fig. 2·2 (c)

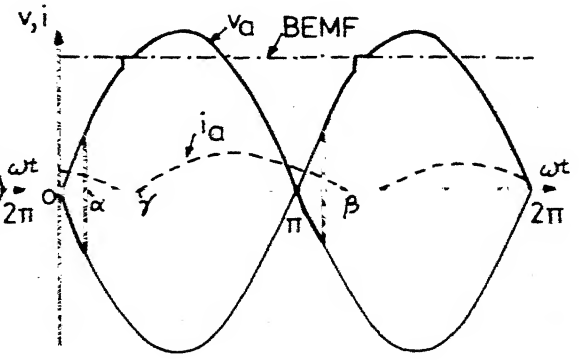

Fig. 2·3(a)

Modes of converter operation

The modes reported earlier [6], [1] for the continuous and discontinuous armature current conduction are shown in Fig. 2.2, It was believed that owing to the back emf of the motor, the incoming thyristor pair cannot be turned on before the instantaneous alternating voltage becomes greater than the back emf [6]. Later, Mehta and Mukhopadhyay [5] showed that the incoming thyristor could be turned on even when the firing angle α is less than γ, the angle at which instantaneous source voltage equals back emf. Thus, they introduced two more modes of operation shown in Fig. 2.3. In addition another mode was identified in inversion operation as shown in Fig. 2.4(a).

In Fig. 2.2(a) $\alpha>\gamma$ hence the incoming pair of thyristors turns on at $\omega t=\alpha$ and conduction ceases at $\omega t=\beta$, where $\beta<(\pi+\alpha)$. In Fig. 2.2(b) $\alpha<\gamma$ hence thyristors turn on at $\omega t=\gamma$, where $\beta<(\pi+\alpha)$ in this case also. Fig. 2.2(c) shows continuous conduction mode of operation with $\alpha>\gamma$.

In Fig. 2.3(a), the armature current has not gone to zero at $\omega t=\pi+\alpha$. The presence of the armature current keeps the incoming thyristors forward biased and they turn on on the application of the gate pulse at $\omega t=\alpha$. The output voltage follows the supply voltage. Since, the back emf is greater than the supply voltage, it oppores the armature current conduction. Current decays to zero at $\omega t=\beta$, where $\beta<\gamma$. Fig. 2.3(b) shows the continuous conduction mode with $\alpha<\gamma$.

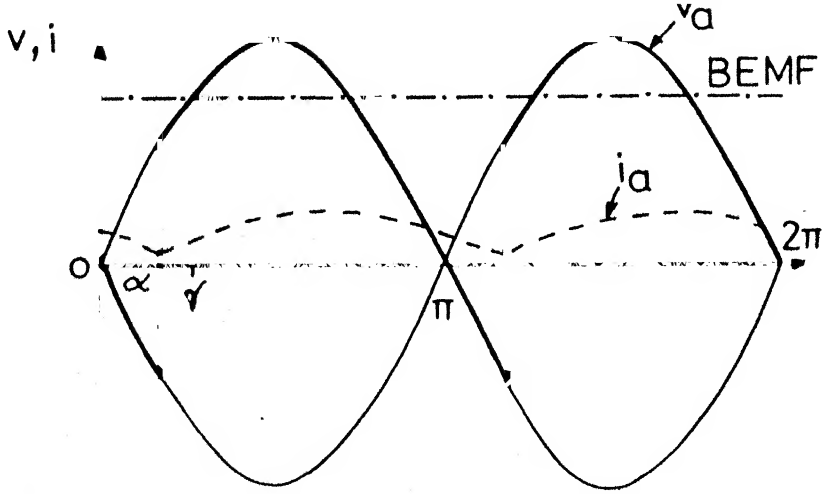

Fig. 2·3(b)

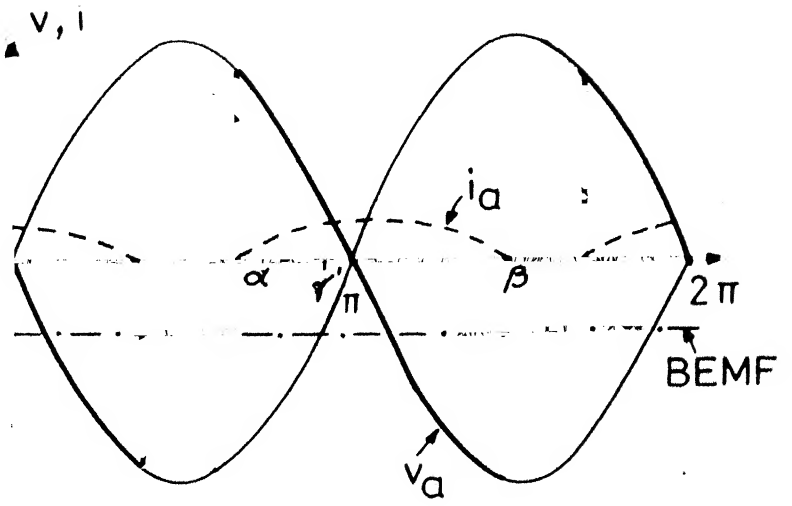

Fig. 2·4(a)

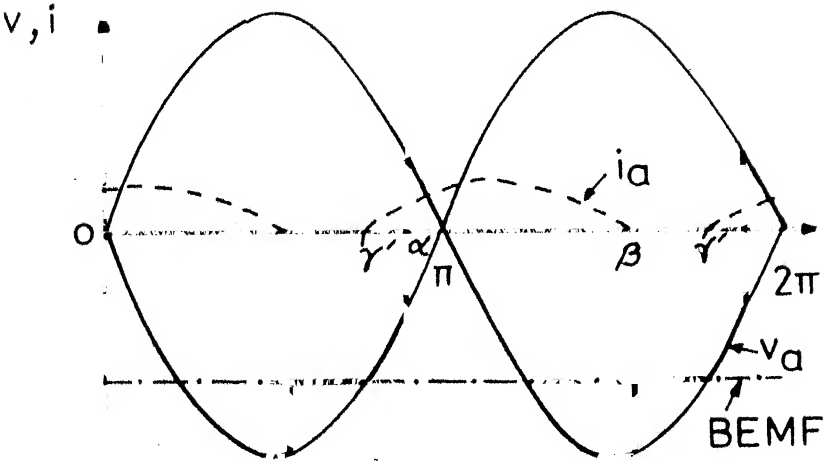

Fig. 2·4(b)

Modes of converter operation

Subbiah and Palanichamy [7] identified a discontinuous conduction mode for inversion shown in Fig.2.4(b), and developed the operating diagram of a single-phase fully controlled converter taking this mode into account.

In Fig. 2.4(a) the incoming pair of thyristors is turned on at $\omega t=\alpha$ and continues to conduct upto $\omega t=\beta$. In Fig. 2.4(b) gating signals are made available for a duration of π radians. For $\alpha=\gamma'$, where $\gamma'=\pi-\gamma$ the current in outgoing pair of thyristors falls to zero at $\omega t=\beta$. These thyristors become forward biased at $\omega t=\gamma$ since firing pulses are present for these thyristors, they regain conduction at $\omega t=\gamma$ and output voltage follows the supply voltage. At $\omega t=\alpha$ incoming pair of thyristors are triggered thereby turning off the outgoing pair.

2.2 CHOICE OF FILTER INDUCTANCE:

The discontinuous armature current operation is undesirable for the following reasons [4].

1. It creates difficulty in commutation of the dc motor.
2. It introduces harmonics in the ac supply.
3. The power factor becomes poor
4. The speed regulation deteriorates and the efficiency of the motor decreases.

Therefore, continuous armature current is desirable even at the smallest possible load. Often, an inductor is inserted in series with the armature circuit to make the armature current continuous. A method was suggested in reference [8] which explained the calculation of minimum inductance necessary in the armature circuit to make the current continuous. But, this method does not work for entire range of rectifier operation. In other words, the method described is valid within specified range of α. The method has been extended by Mehta and Mukhopadhyay [5] to cover the full range of rectifier operation. Subbiah and Palanichamy [7] carried out the calculation for full range of line commutated inverter operation with the help of operating diagram of converter. Later, Anjaneyulu et.al.[9] presented a modified method to optimize the filter inductance. The calculation of the minimum filter inductance has also been discussed by Patel and Doradla [10] and Bhat and Dubey [11] for controlled flywheeling in fully controlled single phase converter. A method to evaluate filter inductance presented in [10] and [11] is suitable for both rectification and inversion.

2.3 SEPARATELY EXCITED DC MOTOR FED BY SINGLE PHASE FULLY CONTROLLED CONVERTER WITH SOURCE INDUCTANCE:

If the current is present in armature circuit at the instant of firing of the incoming pair of thyristors, some finite time is required to commutate the outgoing thyristors. This is called commutation interval or overlap angle. During this period all four thyristors conduct and the thyristor bridge remains shorted. This is explained in Chapter 3. The commutation process gives rise to different modes of operation discussed in Chapter 3.

El-Bolock and Shepherd [12] have analysed the performance of a separately excited dc motor fed by single-phase half controlled converter with finite source inductance present in ac supply. The analysis was reported for continuous mode of operation.

Normally, discontinuous mode of operation cannot be avoided in a dc motor fed by a single-phase converter unless very large external inductance is connected. Since a very large inductance is undesirable from the consideration of economy, drive efficiency and speed response, the analysis must be carried out for discontinuous armature current operation also. In the subsequent chapters of this thesis, the analysis of a single-phase fully controlled bridge converter-fed separately excited dc motor is presented for continuous and discontinuous armature current operations.

CHAPTER 3

EFFECT OF SOURCE INDUCTANCE ON SINGLE PHASE CONVERTER FED DC MOTOR

The finite source inductance of ac supply affects the performance of a single phase fully controlled converter fed separately excited dc motor, because of the delay introduced in the commutation process. It operates in some new modes which are not present in the absence of the source inductance. It also creates difficulties in ac side of the converter such as giving rise to voltage harmonics and deterioration of power factor. In this chapter the commutation process, the modes of operation of the drive for both motoring and regeneration are described for a single-phase converter fed dc separately excited motor. AC supply is assumed to have finite inductance. The system differential equations are solved, and the performance is determined. The steps involved to identify the modes and to evaluate the performance of the drive are given in a flow-chart.

3.1 EFFECT OF SOURCE INDUCTANCE ON WORKING OF CONVERTER:

Consider the full bridge converter in Fig. 3.1. Let us assume that the thyristor pair T_2, T_4 is carrying armature

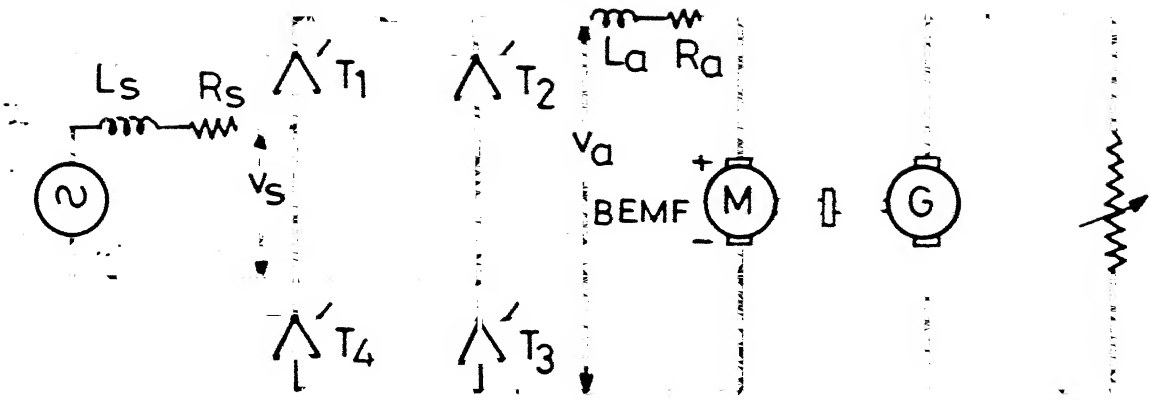

Fig.3·1 Converter fed separately excited dc motor

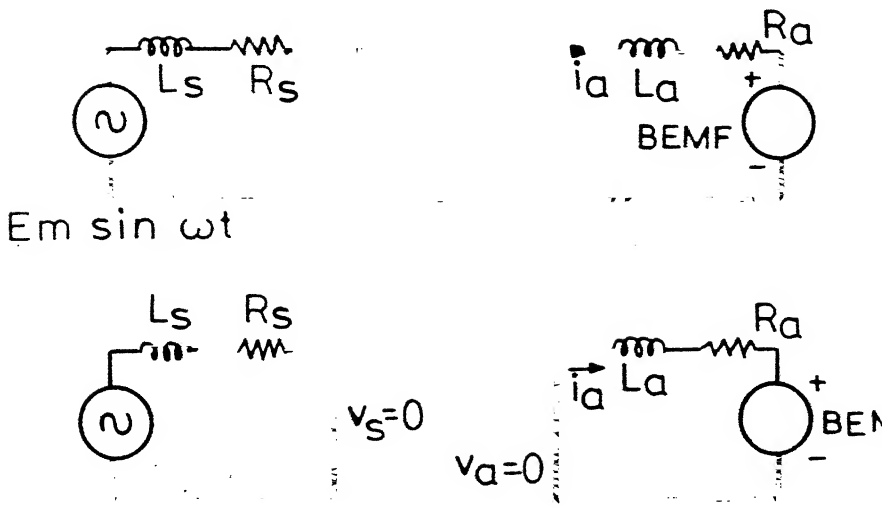

Fig. 3·2 Equivalent circuit

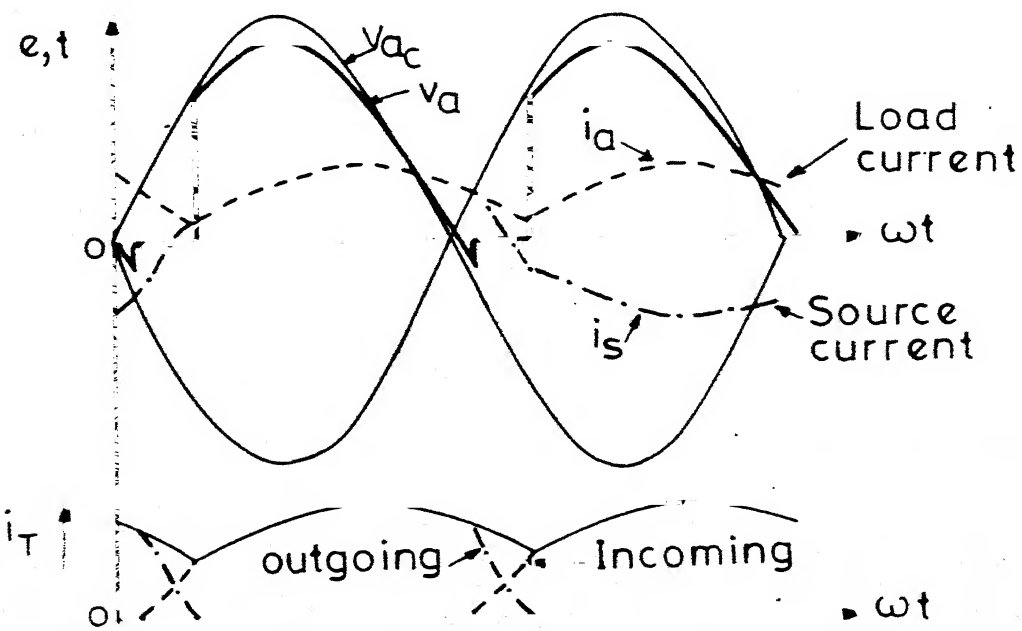

current before $\omega t=\alpha$ in the positive half cycle of the supply voltage. At the instant $\omega t=\alpha$ the instantaneous values of the source current is equal to the instantaneous value of armature current. Since, the thyristor pair T_1,T_3 is forward biased, these thyristors start conducting soon after the application of the gate pulses at $\omega t=\alpha$. It takes finite time called 'commutation interval' or 'overlap angle' for complete transfer of current from T_2,T_4 to T_1,T_3 due to the source inductance. During this interval all the four thyristors conduct and the bridge is completely shorted. The armature current and voltage waveforms are depicted in Fig. 3.3 for this interval. The load current freewheels as shown in Fig.3.2 and the source current flows in the circuit shown in Fig. 3.2. The ac current at the begining of the overlap is given as

$$i_s = -i_a \quad \text{at } \omega t = \alpha \tag{3.1}$$

$$i_s = i_a \quad \text{at } \omega t = \pi+\alpha \tag{3.2}$$

Commutation is completed at the instants given below:

$$i_s = i_a \quad \text{at } \omega t = \mu \tag{3.3}$$

$$i_s = -i_a \quad \text{at } \omega t = \pi+\mu \tag{3.4}$$

or $$i_a = 0 \tag{3.5}$$

The governing equation for the source and load currents during the overlap period are

$$0 = R_a i_a + L_a \frac{di_a}{dt} + \text{BEMF} \qquad (3.6)$$

$$E_m \sin\omega t = R_s i_s + L_s \frac{di_s}{dt} \qquad (3.7)$$

After the commutation interval, the output voltage of the converter is clamped, either to BEMF if $i_a = 0$ or is equal to the ac voltage minus the drop across the source inductance. The waveforms of thyristor currents, during commutation are shown in Fig. 3.3.Considering the commutation process, the converter may operate in any one of the modes described below.

3.2 MODES OF OPERATION DURING RECTIFICATION:

3.2.1 Mode- 1 and 2:

These are continuous conduction mode. The armature current is greater than zero throughout the cycle. At the instant $\omega t=\alpha$ a pair of thyristors T_1, T_3 is fired and the source remain shorted till the current is completely transferred from the outgoing to incoming pair of thyristors. Commutation ends at $\omega t=\mu$. The incoming thyristor pair

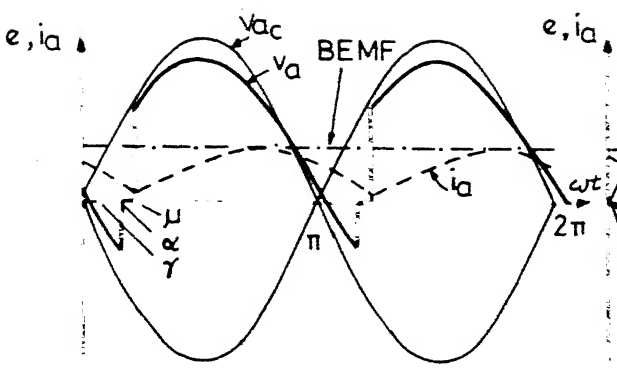

Fig.3·4a MODE 1

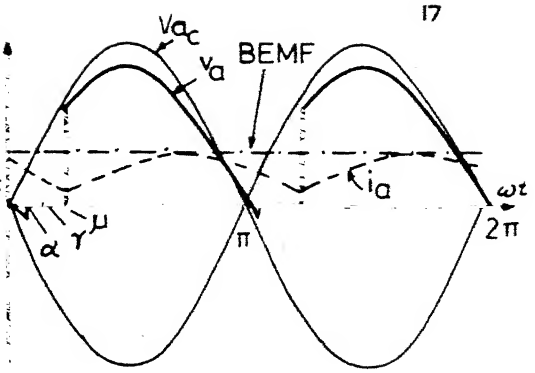

Fig.3·4b MODE 2

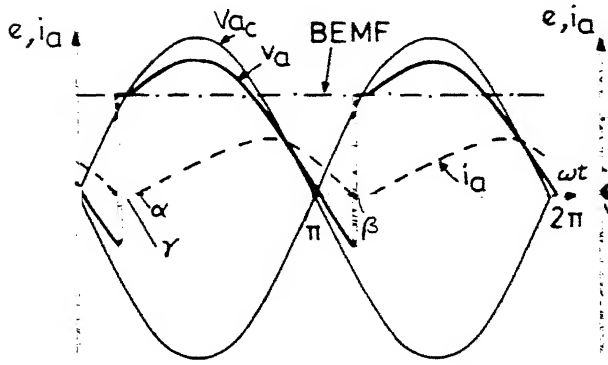

Fig.3·5a MODE 3

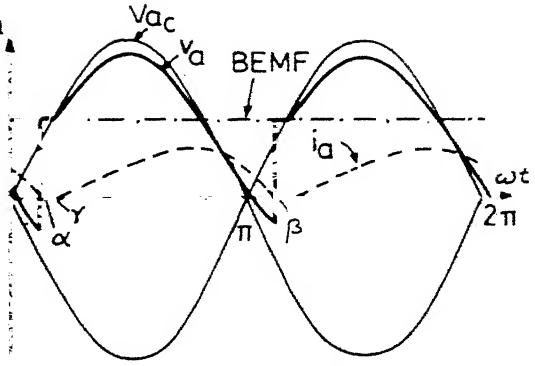

Fig.3·5b MODE 4

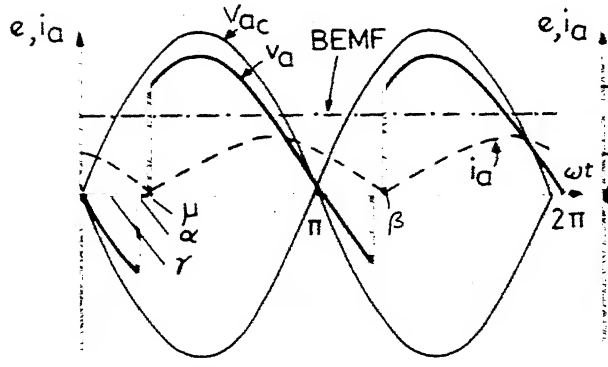

Fig.3·6a MODE 5

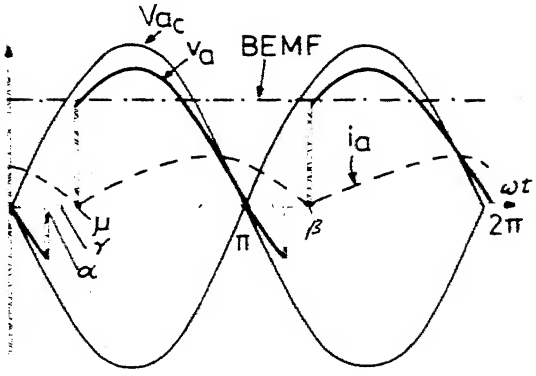

Fig.3·6b MODE 6

turns on at $\omega t=\alpha$ even when $\alpha<\gamma$ since continuous flow of current keeps them forward biased. Mode 11 is for $\alpha>\gamma$ shown in Fig. 3.4(a) and mode 12 is for $\alpha<\gamma$ shown in Fig. 3.4(b).

3.2.2 Mode 3 and 4:

In this mode the current decays to zero at $\omega t=\beta$, where $\beta < (\pi+\alpha)$. If $\alpha<\gamma$ then the conduction commences at $\omega t=\gamma$ since, the back emf keeps the incoming thyristors reverse biased till $\omega t=\gamma$. The output current and voltage waveforms are shown in Fig. 3.5(a) for Mode 3 and in Fig. 3.5(b) for Mode 4.

3.2.3 Mode 5 and 6:

In this mode the armature current falls to zero during commutation at $\omega t=\mu$, however, $\mu>\gamma$. Therefore, the incoming pair of thyristors is forward biased and they regain conduction at $\omega t=\mu$. Fig. 3.6(a) shows mode5 , where $\alpha>\gamma$ and Fig. 3.6(b) shows mode6 , where $\alpha<\gamma$. But in both cases $\mu > \gamma$.

3.2.4 Mode 7:

The armature current falls to zero during the commutation at $\omega t=\mu$. However $\mu<\gamma$. For $\omega t<\gamma$, the instantaneous ac voltage is less than the back emf, the incoming

turns on at $\omega t=\alpha$ even when $\alpha<\gamma$ since continuous flow of current keeps them forward biased. Mode 11 is for $\alpha>\gamma$ shown in Fig. 3.4(a) and mode 12 is for $\alpha<\gamma$ shown in Fig. 3.4(b).

3.2.2 Mode 3 and 4:

In this mode the current decays to zero at $\omega t=\beta$, where $\beta < (\pi+\alpha)$. If $\alpha<\gamma$ then the conduction commences at $\omega t=\gamma$ since, the back emf keeps the incoming thyristors reverse biased till $\omega t=\gamma$. The output current and voltage waveforms are shown in Fig. 3.5(a) for Mode 3 and in Fig. 3.5(b) for Mode 4.

3.2.3 Mode 5 and 6:

In this mode the armature current falls to zero during commutation at $\omega t=\mu$, however, $\mu>\gamma$. Therefore, the incoming pair of thyristors is forward biased and they regain conduction at $\omega t=\mu$. Fig. 3.6(a) shows mode5 , where $\alpha>\gamma$ and Fig. 3.6(b) shows mode6 , where $\alpha<\gamma$. But in both cases $\mu > \gamma$.

3.2.4 Mode 7:

The armature current falls to zero during the commutation at $\omega t=\mu$. However $\mu<\gamma$. For $\omega t<\gamma$, the instantaneous ac voltage is less than the back emf, the incoming

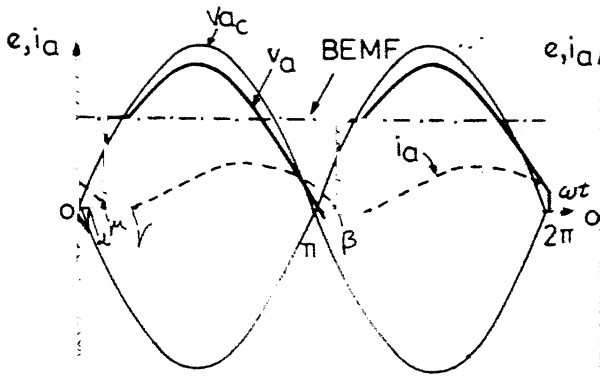

Fig. 3·7 MODE 7

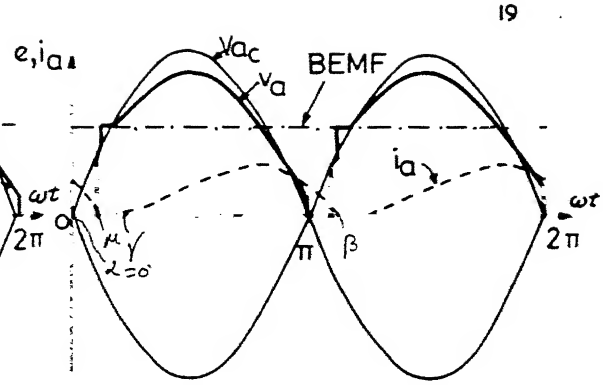

Fig. 3·8 MODE 8

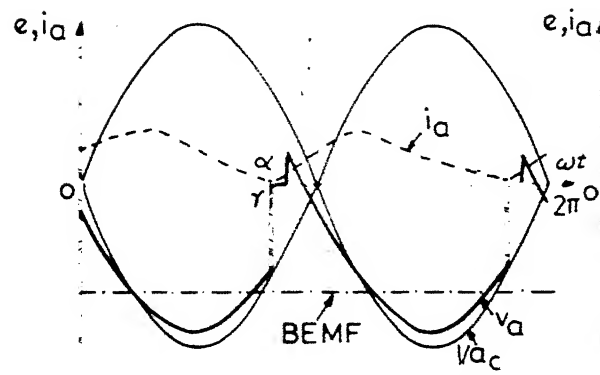

Fig. 3·9(a) MODE 1

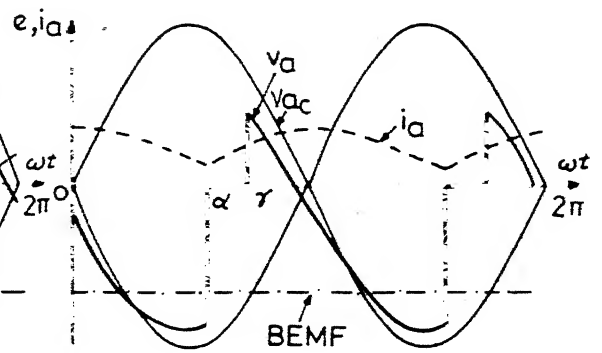

Fig. 3·9(b) MODE 2

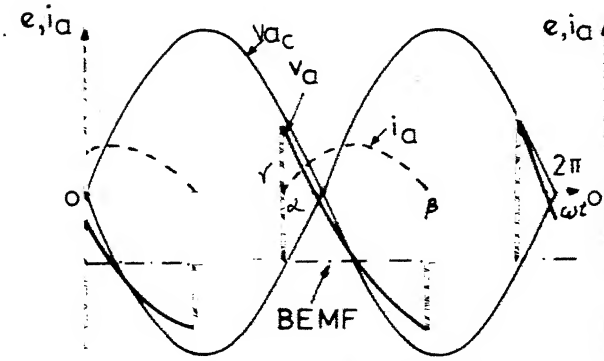

Fig. 3·10 MODE 3

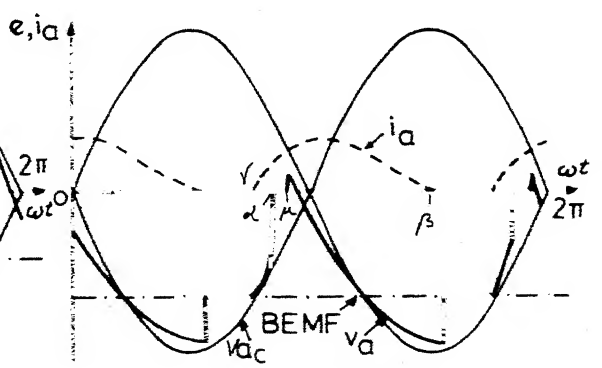

Fig. 3·11 MODE 4

thyristors remain reverse biased till $\omega t=\gamma$. Therefore, conduction commences at $\omega t=\gamma$. Output voltage between $\mu \leq \omega t \leq \gamma$ remains clamped to the back emf. Output voltage and current waveforms are shown in Fig. 3.7.

3.2.5 Mode-8:

The armature current falls to zero after commutation is completed. Therefore, $\beta > \mu$. But at $\omega t=\beta$ the instantaneous ac voltage is less than the back emf, hence the incoming thyristors will turn on only at $\omega t=\gamma$. The output voltage remains zero during the commutation and becomes equal to the instantaneous ac voltage minus the drop across the source inductance after commutation. For $\beta \leq \omega t \leq \gamma$, the output voltage is equal to the back emf and the armature current is zero. Fig. 3.8 shows the current conduction in mode 8.

3.3 MODES OF OPERATION DURING INVERSION:

For regeneration or inversion motor back emf direction with respect to converter terminals must reverse. This can be obtained by reversal of the direction of rotation of the motor or reversal of the motor connection with respect to the converter or due to field reversal with the direction of

motor rotation remaining unchanged. Therefore, the motor back emf will be negative. Now the supply voltage oppores the flow of the armature current and the motor back emf assists the flow of armature current. In the presence of armature current, thyristor pair T_1,T_3 is forward biased when supply voltage is positive and the other pair of thyristors is forward biased during the next half cycle of the ac voltage. In the absence of armature current and during the negative half cycle thyristors T_2 and T_4 will be forward biased. The different modes of operation are as follows.

3.3.1 Mode 1 and Mode 2:

This is identical to mode one of the rectification operation, except that back emf is negative and $90<\alpha<180$. Fig. 3.9(a) shows the mode 1 where $\alpha>\gamma'$ and Fig. 3.9(b) shows mode 2, where $\alpha<\gamma'$.

3.3.2 Mode 3:

This is again similar to mode3 of the rectification operation. The waveforms are shown in Fig. 3.10. The incoming thyristors are forward biased at any instant throughout the cycle, therefore, they turn on at the instant $\omega t=\alpha$.

3.3.3 Mode 4:

This mode can be obtained by maintaining the firing pulse duration equal to π radians. Here $\alpha > \gamma$, where $\gamma' = \pi-\gamma$, and armature current falls to zero at $\omega t=\beta$, where $\beta<\gamma'$. Due to the presence of firing pulses, the outgoing thyristor pair regain conduction. Since, they become forward biased at $\omega t=\gamma'$ again. At $\omega t=\alpha$ the incoming thyristor pair is fired and commutation takes place. The current transfer is completed from outgoing to incoming thyristor pair at $\omega t=\mu$. The current and voltage waveforms are shown in Fig. 3.11.

3.4 SYSTEM REPRESENTATION:

The circuit in Fig. 3.1 shows the system under consideration. This is analysed subjected to the following assumption.

1. The thyristors are ideal switches
2. AC source has significant internal inductance which is assumed lumped parameter between ideal voltage source and mains. This remains constant throughout the operation.
3. Under steady state conditions the motor speed is constant.

4. The resistance and reactance of the armature circuit remain unchanged throughout the operation.
5. All the angles are measured from natural zero crossing of the pure sine wave of ac voltage.
6. Firing is symmetrical.

Fig. 3.1 and Fig. 3.2 show the converter system under consideration and its equivalent circuit. The voltage source is an ideal voltage source behind internal impedance. The motor is represented by R-L load with back emf. The set of equations expressing source and armature currents, during commutation and normal operation, for different modes are as follows.

3.4.1 Rectifier Operation:

Mode 1 and 2:

$$E_m \sin\omega t = L \frac{di_a}{dt} + Ri_a + BEMF \qquad (3.9)$$

$$o \leq \omega t < \alpha$$

$$E_m \sin\omega t = L_s \frac{di_s}{dt} + R_s i_s$$

$$\alpha \leq \omega t < \mu \qquad (3.10)$$

and $$O = L_a \frac{di_a}{dt} + R_a i_a + BEMF$$

$$\alpha \leq \omega t < \mu \qquad (3.11)$$

$$E_m \sin\omega t = L \frac{di_a}{dt} + Ri_a + BEMF$$

$$\mu \leq \omega t < \pi \qquad (3.12)$$

where $L = L_a+L_s$; $R = R_a+R_s$; ω supply frequency in rad/sec. Eqns. (3.9) and (3.12) describe normal operation and Eqns. (3.10) and (3.11) are for commutation interval. Since firing is maintained symmetric, only one half cycle is considered and in the next half cycle the eqn. will repeat in the same fashion.

Mode 3,4:

$$E_m \sin\omega t = L \frac{di_a}{dt} + Ri_a + BEMF$$

$$\alpha \leq \omega t < \beta \text{ for mode } 3 \qquad (3.13)$$

$$\gamma \leq \omega t < \beta \text{ for mode } 4$$

$$i_a = 0;\ i_s = 0$$

$$\beta \leq \omega t < \pi+\alpha \text{ for mode } 3$$

$$\beta \leq \omega t < \pi+\gamma \text{ for mode } 4 \qquad (3.14)$$

Mode 5,6:

$$E_m \sin\omega t = L \frac{di_a}{dt} + Ri_a + BEMF$$

$$o \leq \omega t < \alpha \qquad (3.15)$$

$$E_m \sin\omega t = L_s \frac{di_s}{dt} + R_s i_s$$

$$\alpha \leq \omega t < \mu \qquad (3.16)$$

$$0 = L_a \frac{di_a}{dt} + R_a i_a + BEMF$$

$$\alpha \leq \omega t < \mu \qquad (3.17)$$

Eqn. (3.15) repeats during $\mu \leq \omega t \leq \pi$.

Mode 7:

$$E_m \sin\omega t = L \frac{di_a}{dt} + Ri_a + BEMF$$

$$o \leq \omega t < \alpha \qquad (3.18)$$

$$E_m \sin\omega t = L_s \frac{di_s}{dt} + R_s i_s$$

$$\alpha \leq \omega t < \mu \qquad (3.19)$$

$$0 = L_a \frac{di_a}{dt} + R_a i_a + BEMF$$

$$\alpha \leq \omega t < \mu \qquad (3.20)$$

$$i_a = 0;\ i_s = 0 \qquad \mu \leq \omega t < \gamma \qquad (3.21)$$

Equation (3.18) repeats between $\gamma \leq \omega t \leq \pi$.

Mode 8:

$$E_m \sin\omega t = L \frac{di_a}{dt} + Ri_a + BEMF$$

$$o \leq \omega t < \alpha \qquad (3.22)$$

$$E_m \sin\omega t = L_s \frac{di_s}{dt} + R_s i_s$$

$$\alpha \leq \omega t < \mu \qquad (3.23)$$

$$0 = L_a \frac{di_a}{dt} + R_a i_a + BEMF$$

$$\alpha \leq \omega t < \mu \qquad (3.24)$$

$$i_a = 0;\ i_s = 0 \qquad \mu \leq \omega t < \gamma \qquad (3.25)$$

Equation (3.22) repeats between $\gamma \leq \omega t < \pi$.

3.4.2 Inversion:

For inversion or regeneration the following conditions are to be satisfied

1. $90 < \alpha < 180$
2. Back emf is negative or its direction is reversed.

The equations describing the mode of operation are as follows.

Mode 1 and Mode 2:
Mode 3

These equations are same as the corresponding modes in rectifier operation with the above two conditions satisfied.

Mode 4:

$$E_m \sin\omega t = L \frac{di_a}{dt} + Ri_a + BEMF \qquad \gamma' \leq \omega t < \alpha \qquad (3.26)$$

$$0 = L_a \frac{di_a}{dt} + R_a i_a + BEMF \qquad \alpha \leq \omega t \leq \mu \qquad (3.27)$$

$$E_m \sin\omega t = L_s \frac{di_s}{dt} + R_s i_s \qquad \alpha \leq \omega t < \mu \qquad (3.28)$$

$$E_m \sin\omega t = L \frac{di_a}{dt} + Ri_a + BEMF \qquad \mu \leq \omega t < \beta \qquad (3.29)$$

$$i_a,\ i_s = 0 \qquad \beta \leq \omega t < \gamma' \qquad (3.30)$$

3.5 PERFORMANCE EVALUATION:

The above set of equations, for different modes, are solved numerically to evaluate the performance of the drive. Fourth order Runge-Kutta method has been used in the program.

To evaluate the Fourier-coefficients, few samples of values of source current is taken at the end of each step and integrated numerically as follows.

The Fourier coefficients a_n and b_n are defined as

$$a_n = \frac{1}{\pi} \int_0^{2\pi} f(x)\cos n\omega t \, dt \qquad (3.31)$$

$$b_n = \frac{1}{\pi} \int_0^{2\pi} f(x) \sin n\omega t \, dt \qquad (3.32)$$

here, $f(x) = i_s$. Let i_k denote the descrete values of i_s at kth step then above integration is replaced by the following summation.

$$a_n = \frac{1}{\pi} \sum_{k=1}^{N} (i_k \cos n\omega t_k).(h) \qquad n = 1,2,3,... \qquad (3.33)$$

$$b_n = \frac{1}{\pi} \sum_{k=1}^{N} (i_k . \sin n\omega t_k).(h) \qquad n=1,2,3,... \qquad (3.34)$$

Similarly, coefficients for input voltage to converter v_s are calculated. The fundamental component is calculated by putting n=1. The fundamental RMS values are given by For current

$$i_{s1(RMS)} = (a_1^2 + b_1^2)^{1/2} \qquad (3.35)$$

and its phase angle is given by

$$\phi_I = \tan^{-1} \frac{b_1}{a_1} \qquad (3.36)$$

Similarly for voltage

$$V_{s1(RMS)} = (a_1^2 + b_1^2)^{1/2} \qquad (3.37)$$

and

$$\phi_V = \tan^{-1} \frac{b_1}{a_1} \qquad (3.38)$$

The overall RMS value of voltage and current is calculated as follows.

$$I_{s(RMS)} = [\frac{1}{2\pi} (\sum_{k=1}^{N} i_k^2 . h)]^{1/2} \qquad (3.39)$$

$$V_{s(RMS)} = [\frac{1}{2\pi} (\sum_{k=1}^{N} v_k^2 . h)]^{1/2} \qquad (3.40)$$

Now distortion factors and displacement factor are calculated as follows.

$$\text{Current distortion factor (IDISF)} = \frac{I_{s1(RMS)}}{I_{s(RMS)}} \qquad (3.41)$$

$$\text{Voltage distortion factor (VDISF)} = \frac{V_{s1(RMS)}}{V_{s(RMS)}} \qquad (3.42)$$

$$\text{Displacement factor (DISPF)} = \cos(\phi_V - \phi_I) \qquad (3.43)$$

$$\text{Power factor} = (\text{IDISTF}).(\text{VDISTF}).(\text{DISPF}) \qquad (3.44)$$

3.5.2 Mode Identification:

Knowing the loading conditions, motor parameters and ac source parameters, first of all the relevant mode is identified and then the calculation for that particular mode is completed. For an assumed steady state speed, value of armature current is assumed to be for the steady state if the instantaneous values of armature current at the begining and at the end of a half cycle are equal. If current is discontinuous and conduction period is less than π rad. then steady state value is obtained in one half cycle only. If conduction period is equal to π, computation over

few cycles may be necessary for obtaining the steady state solution. To calculate the average quantity, few samples of instantaneous values, over the whole cycle, are taken and multiplied by the step length. The average of these products gives the average value of the relevant quantity.

3.6 FLOW CHART:

The flow chart shown in Fig. 3.12 discribes the steps used to develop the program to identify the modes and to calculate speed torque characteristics of the motor.

The input quantities are firing angle, armature circuit parameters, ac source parameters, back emf constant and torque constant. In the program, the first step is to choose the step-length, calculate back emf, γ and initialize $\omega t=\alpha$. If α is less than γ then ωtiis set equal to γ.

Now equation (3.9) for the normal operation is solved numerically at successive steps and every time the value of armature current is checked. If it falls to zero then it is mode 2 otherwise solution is repeated till $\omega t=\pi+\alpha$. Armature current values at $\omega t=\alpha$ and $\omega t=\pi+\alpha$ must be same in the steady state. Therefore, Eqns. (3.10) and (3.11) are solved till $\omega t=\mu$. If armature current falls to zero during commutation process and $\mu<\gamma$ then it is mode 4. Otherwise Eqn. (3.9) is

solved after commutation ends. If armature current falls to zero before $\omega t=\gamma$ then it is mode 5. Otherwise, solution is repeated for next half cycle. This is repeated over a few cycles so the armature current correspond to steady state. Now, again Eqn. (3.10) and (3.11) are solved and armature current is checked if it falls to zero during commutation. If it falls to zero then Mode 3 is obtained otherwise mode 1. If source inductance is zero then solution of equations during commutation process are skipped. Rest all calculations are same.

Once, the mode is identified for given load and firing angle, computation are made to obtain the speed-torque characteristics. The distortion factors displacement factor and power factor are also calculated.

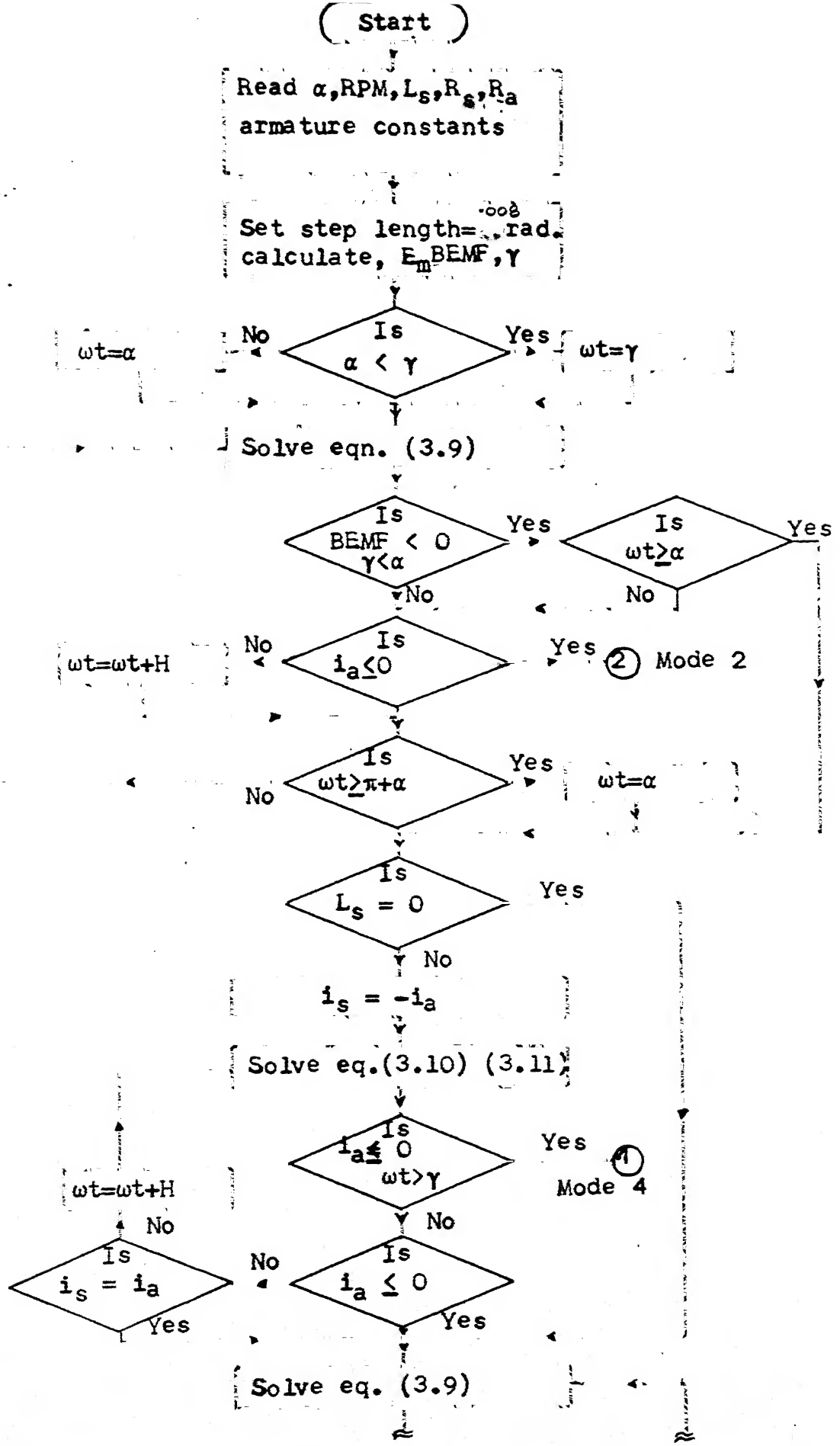

Fig. 3.12 Flow Chart

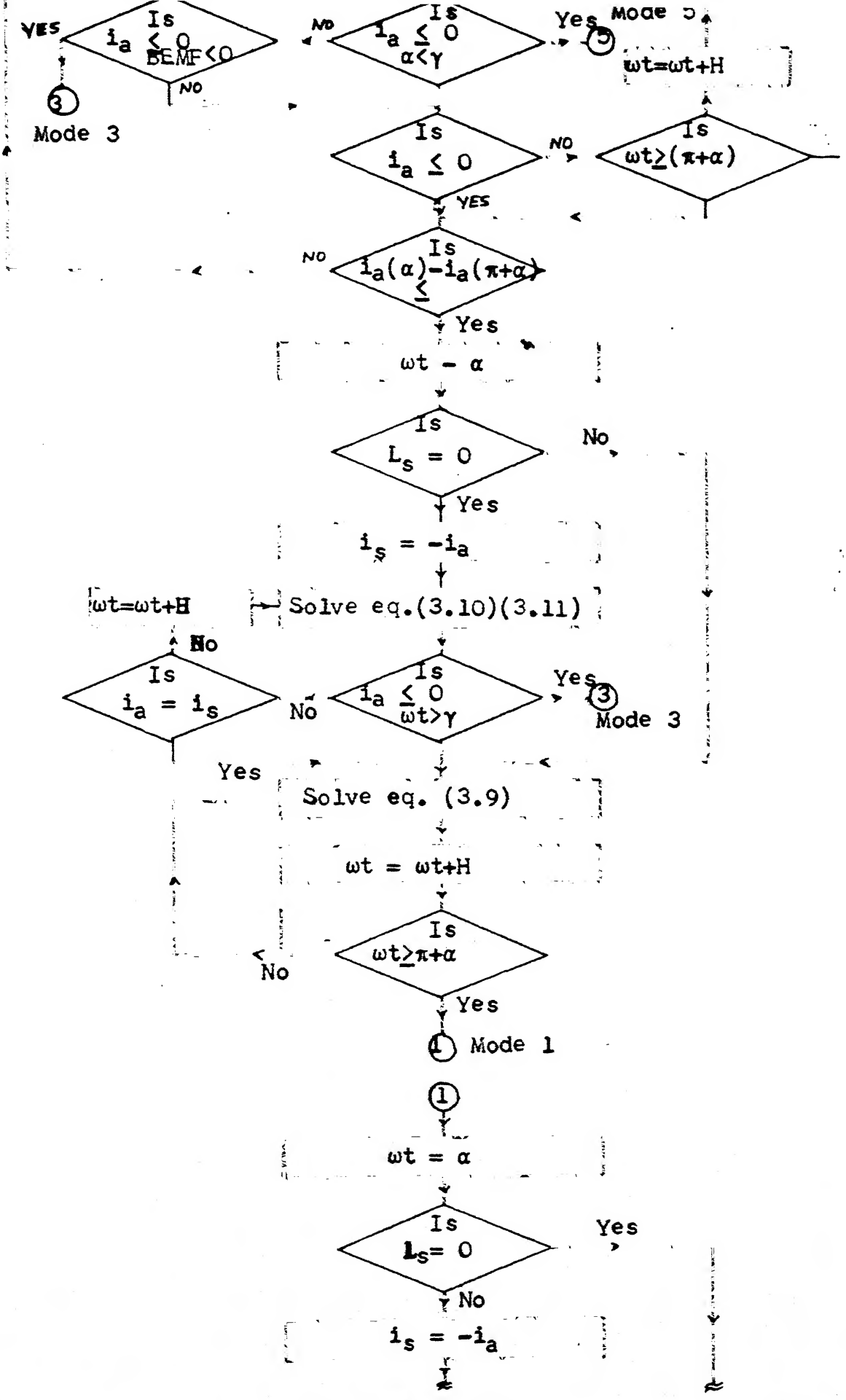

Fig. 3.12 contd

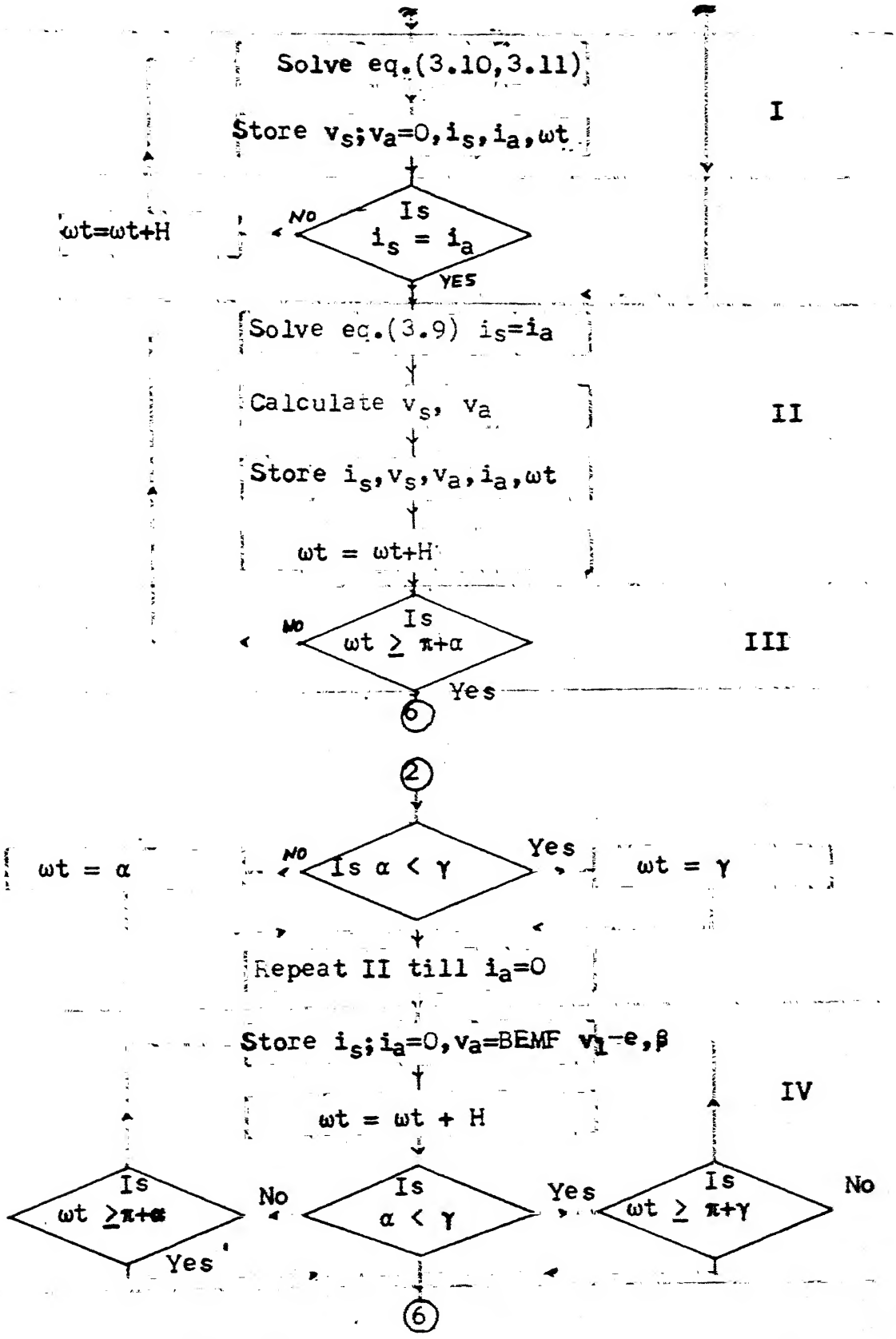

Fig. 3.12 contd.

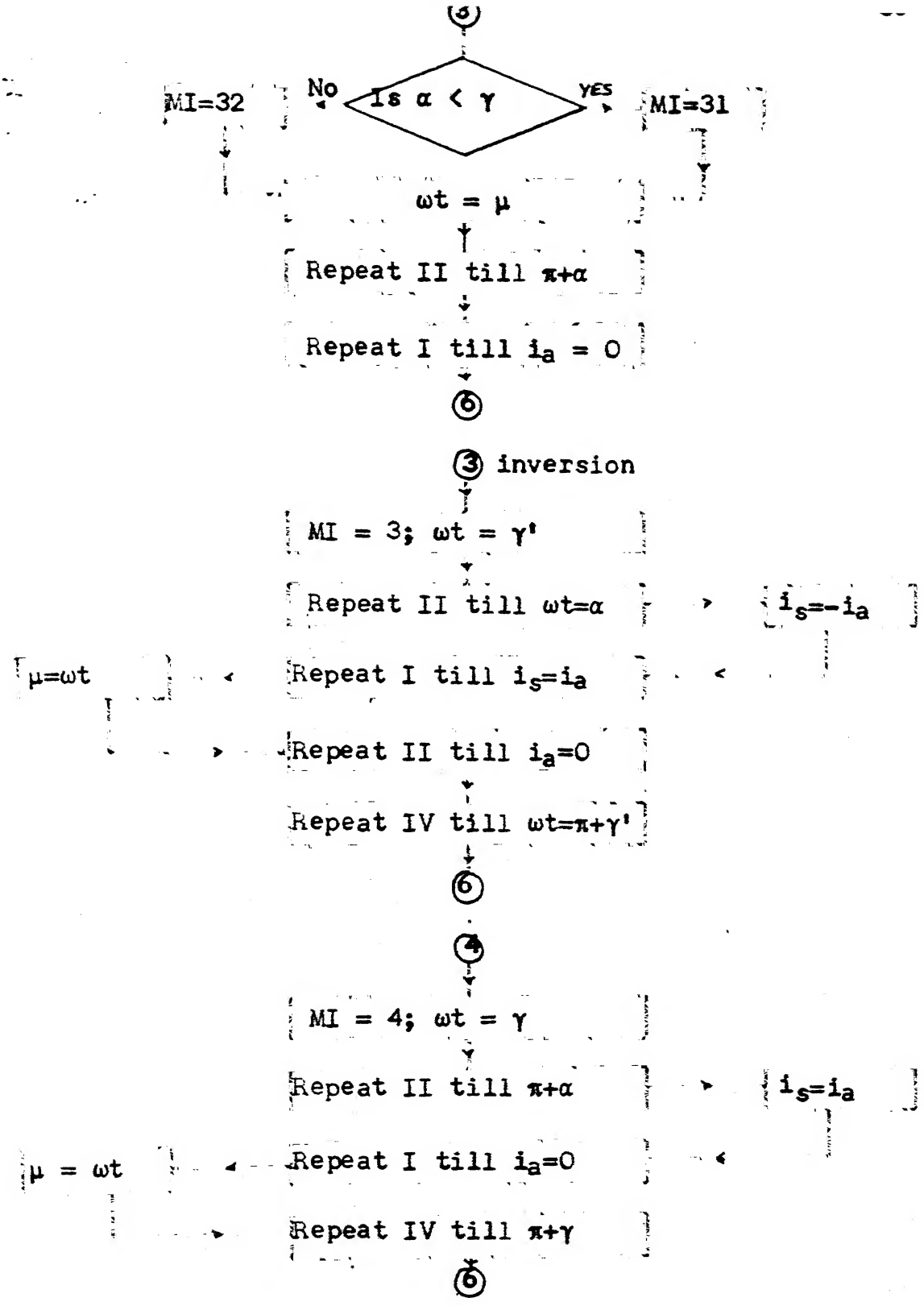

Fig.3.12 contd.

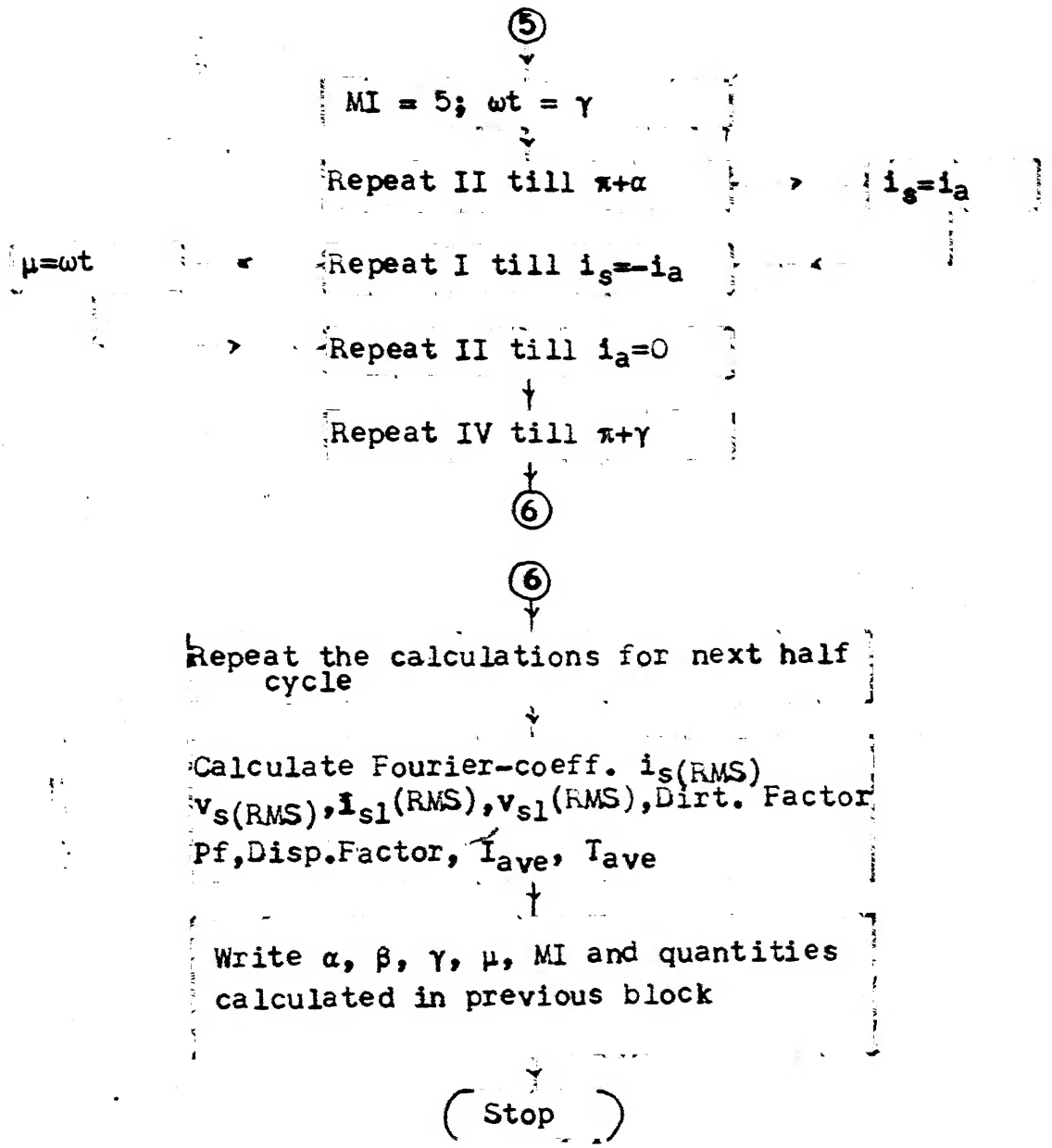

Fig. 3.12 contd..

CHAPTER 4

PERFORMANCE AND EXPERIMENTAL RESULTS

The present chapter describes the drive performance and its experimental verification.

4.1 EXPERIMENTAL SET UP:

The power circuit is shown in Fig. 4.1. The load is a separately excited dc generator which is mechanically coupled to the separately excited dc motor under study. The separately excited dc motor is fed by a single phase fully controlled converter with symmetrical firing. The field is supplied from 220V regulated dc source. The generator is connected to a resistive load.

The thyristor ratings for full bridge converter are chosen such that it feeds the motor at full load. For the purpose of study, an external inductor with tappings, for varying its inductance, is connected in series with the ac source. This simulates an ac source with finite internal inductance, a lumped parameter. The resistance of the inductor has also been taken into account. No extra inductance has been added to the armature circuit so that all the

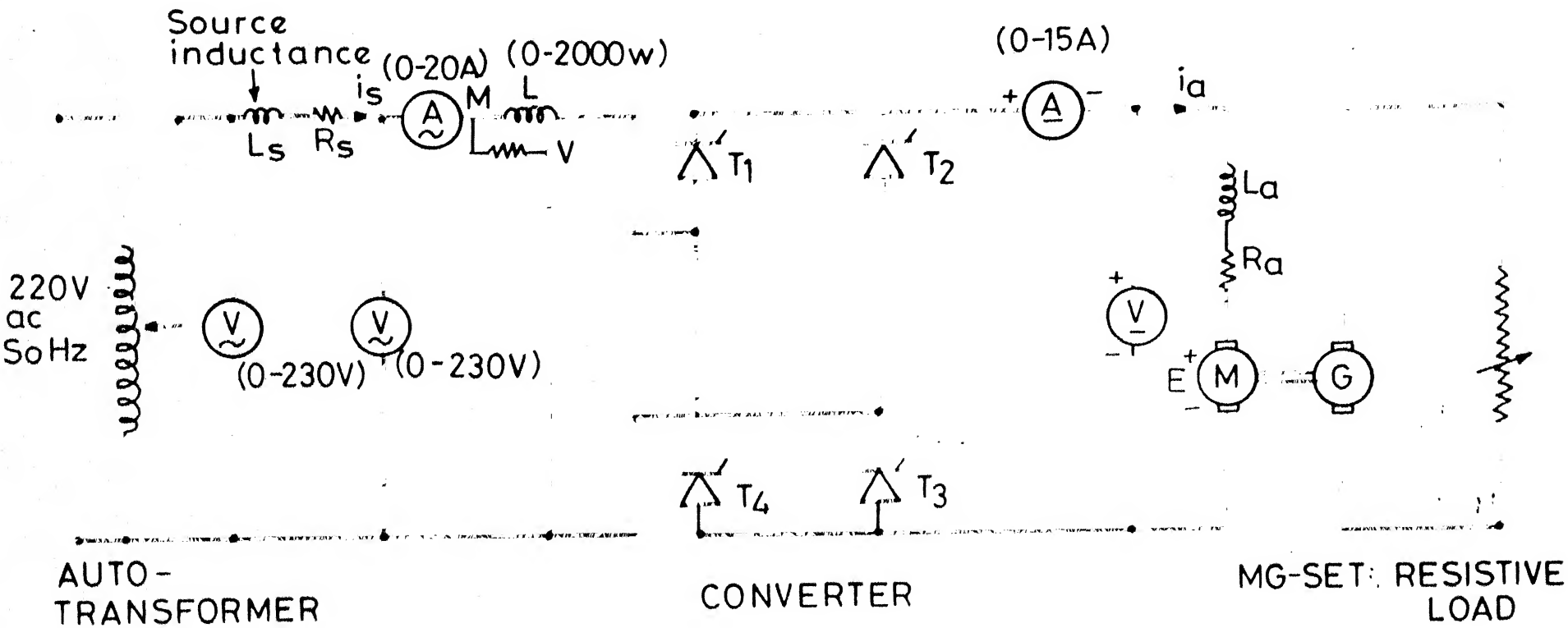

Fig. 4-1 Power circuit diagram

discontinuous modes may be observed as described in Sections 3.2 and 3.3 in this thesis.

Motor back emf constant, torque constant, resistance and inductance have been measured and given in the appendix.

The motor which is used for this study has weak field (due to defect), hence, it reaches its rated speed below rated armature voltage when field is excited with rated voltage. Therefore system operates at reduced voltage.

4.2 FIRING CIRCUIT:

Fig. 4.2 shows the firing circuit used to control the full bridge single phase converter with symmetrical firing. The armature of the circuit is illustrated by pertinant waveform in Fig. 4.4.

In block I, the synchronizing signal is transformed into square wave signal using op-amp 1 and 2. The negative pulse are eliminated by using diodes at the output of each op-amp. A and A' show the waveform at the A and A and A' of the circuit. The op-amp 3 in block II integrate the output waveform of op-amp 1.

The op-amp in block III is used as a summing amplifier and variable dc level is applied to the non-inverting terminal of this op-amp so that the dc level can be adjusted.

The output of this op-amp is then fed to the non-inverting terminals of op-amp 5 in block IV and compared with variable dc voltage fed to the inverting terminal, output of this op-amps5 consists of pulses D. The ramp output of op-amp 4 is inverted by op-amp 7 in inverting mode and is then compared to a dc level to output pulses G.

In block V, the 555 timer is connected in astable mode to give high frequency pulses E. The pulses of pair D and G correspond to $(\pi+\alpha)$ and α respectively. These pulses are ANDed with A and A' so that they extend upto the next zero crossing of the synchronizing signal. These pulses are then modulated with high frequency pulses E in block VII.

The driver stage consists of two transistors in Darlington configuration. The pulses are output through the collector of the transistor and passed through the isolating pulse transformer. The diodes at the secondary of the pulse transformer are to prevent negative excursion of triggering pulses.

4.3 FIRING CIRCUIT II:

Fig. 4.3 shows the firing circuit to produce triggering pulse of duration π rad. The waveforms are shown in Fig. 4.5.

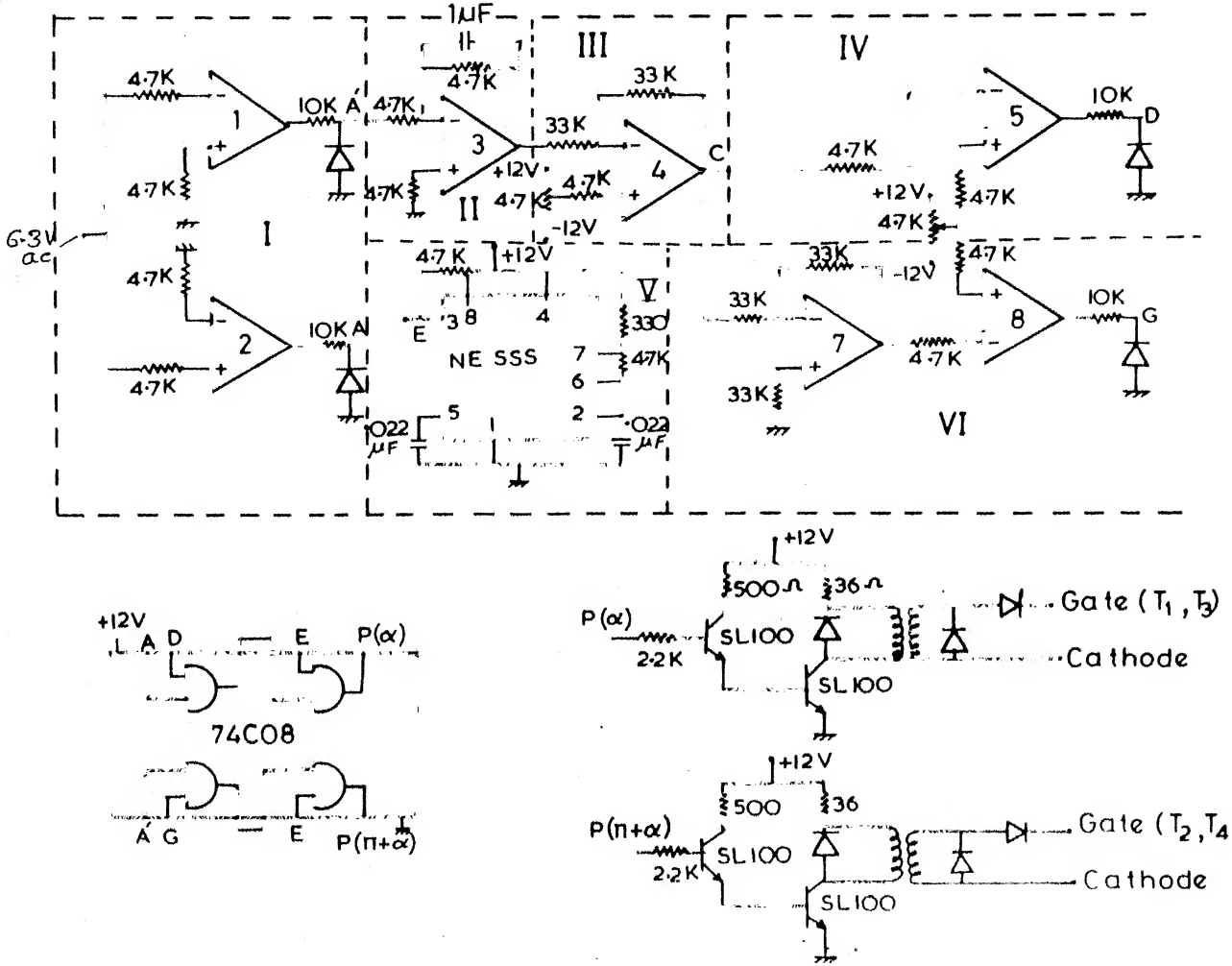

Fig. 4·2 Firing circuit I

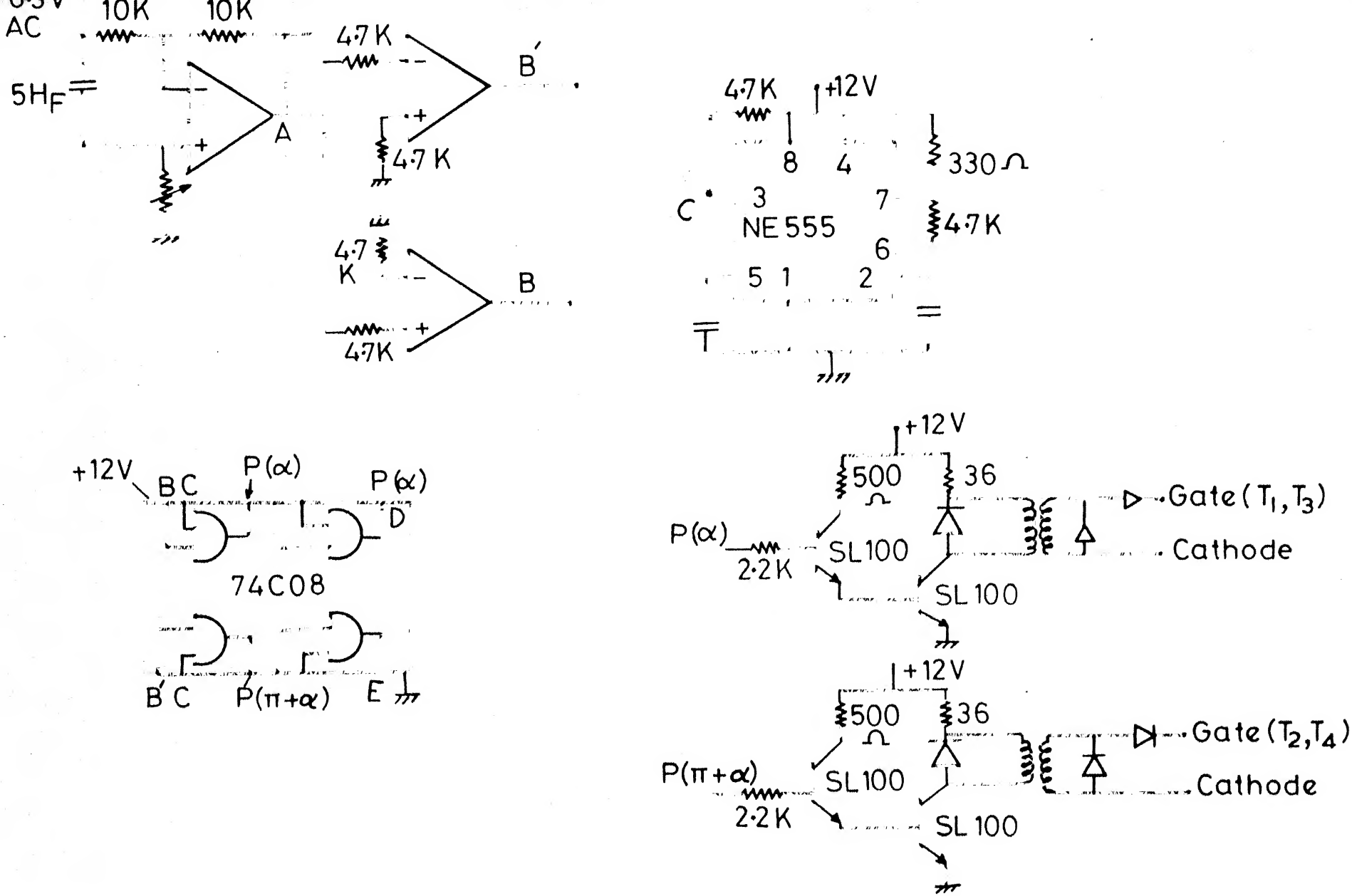

Fig.4·3 Firing circuit-II

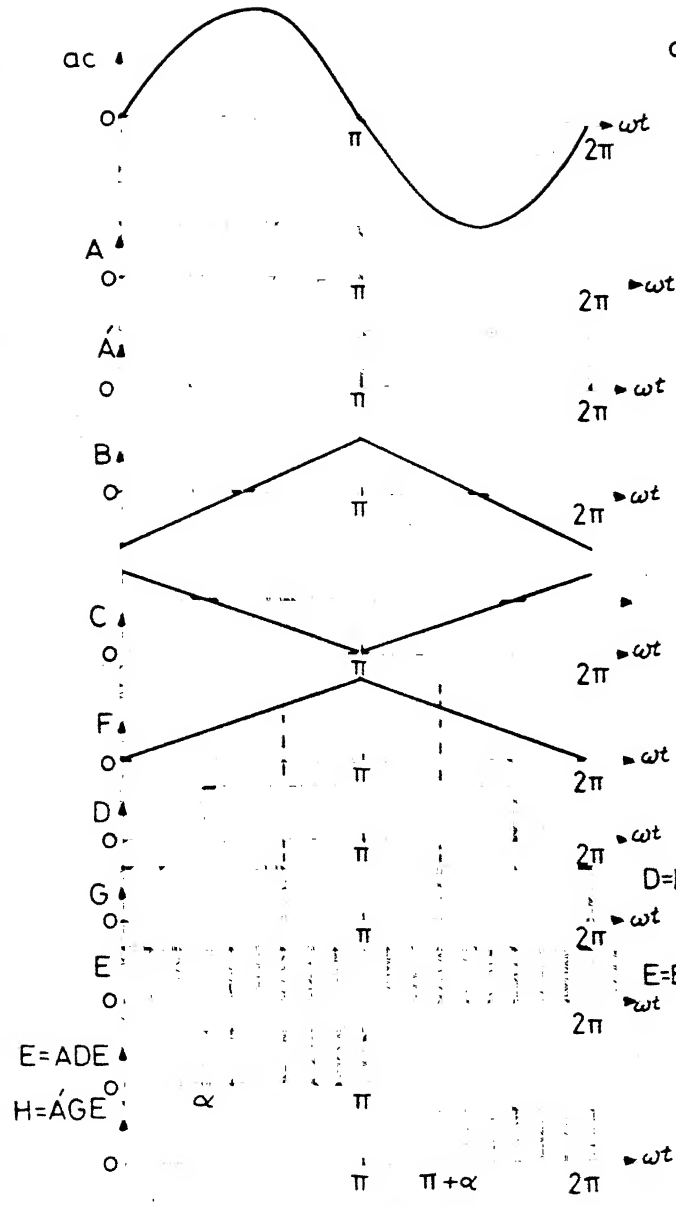

Fig. 4·4

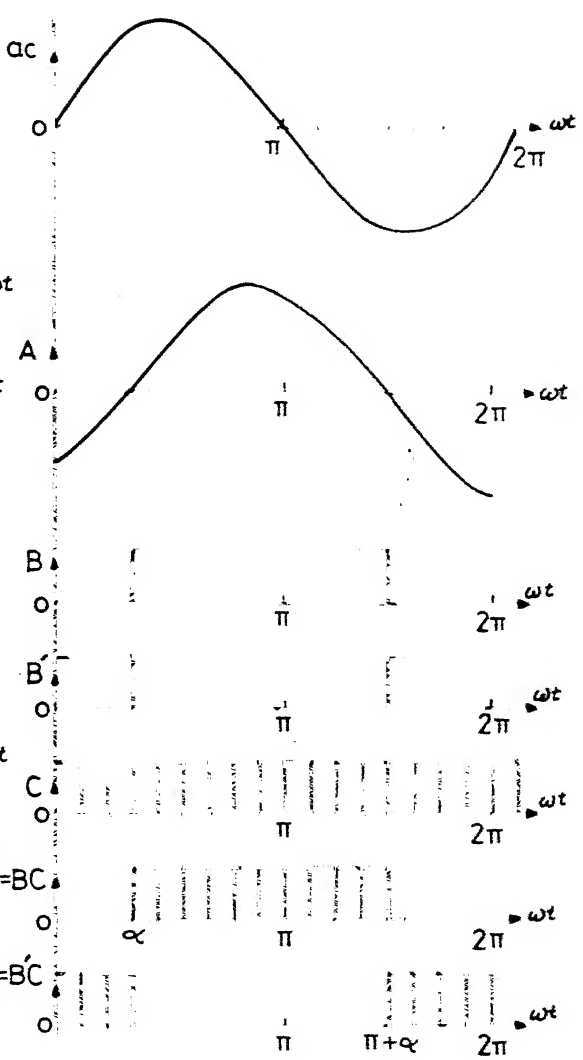

Fig. 4·5

Waveforms at various stages of the circuit

Op-amp 1 is fed by a synchronizing signal. This op-amp is configured in phase shifting mode. The phase shift from O to π rad. can be obtained by adjusting the variable resistance. The phase-shifted synchronizing signal is passed through zero crossing detectors to output waveforms A and A'. These pulses are of duration π rad. Now these pulses are modulated with high frequency pulses. The modulated signal is then passed through driver circuit and pulse transformer as discussed in Section 4.2.

4.4 PERFORMANCE:

Experiment was conducted for both rectification and regeneration. The power circuit shown in Fig. 4.1 is common for both the cases except following conditions are satisfied for regeneration.

1. The direction of back emf and wattmeter connection are reversed for regeneration.
2. The dc generator which was working as load to the motor, now drives the motor which now works as a generator.

Since the modes are dependent on the firing angle and loading condition, these parameters were adjusted to observe

all the modes in rectification and regeneration. These were discussed in Chapter 3. The above two conditions were obtained by theoretical computations and with these, the modes were simulated in the experiment. These modes were photographed for both rectification and regeneration and the oscillograms are presented in Fig. 4.6. All the modes are exactly the same as expected in theory. The mode 5 in rectification and the mode 1 in regeneration could not be observed for the following reason.

According to theoretical calculations, the conditions for mode 5 are zero firing angle, low value of inductance and high speed. To satisfy these requirement was not possible in the present experimental setup, hence mode 5 of rectification could not be observed.

During regeneration, efforts were made to adjust the parameters to obtain both the modes in continuous conduction. But commutation failure was found to occur even at the slight change of either of the two parameters. Therefore, only one of the two modes in continuous conduction could be observed.

Speed-torque characteristics have been computed for various values of firing angles and source inductance. The characteristics are shown in Figs. 4.7, 4.8, 4.9 and 4.10.

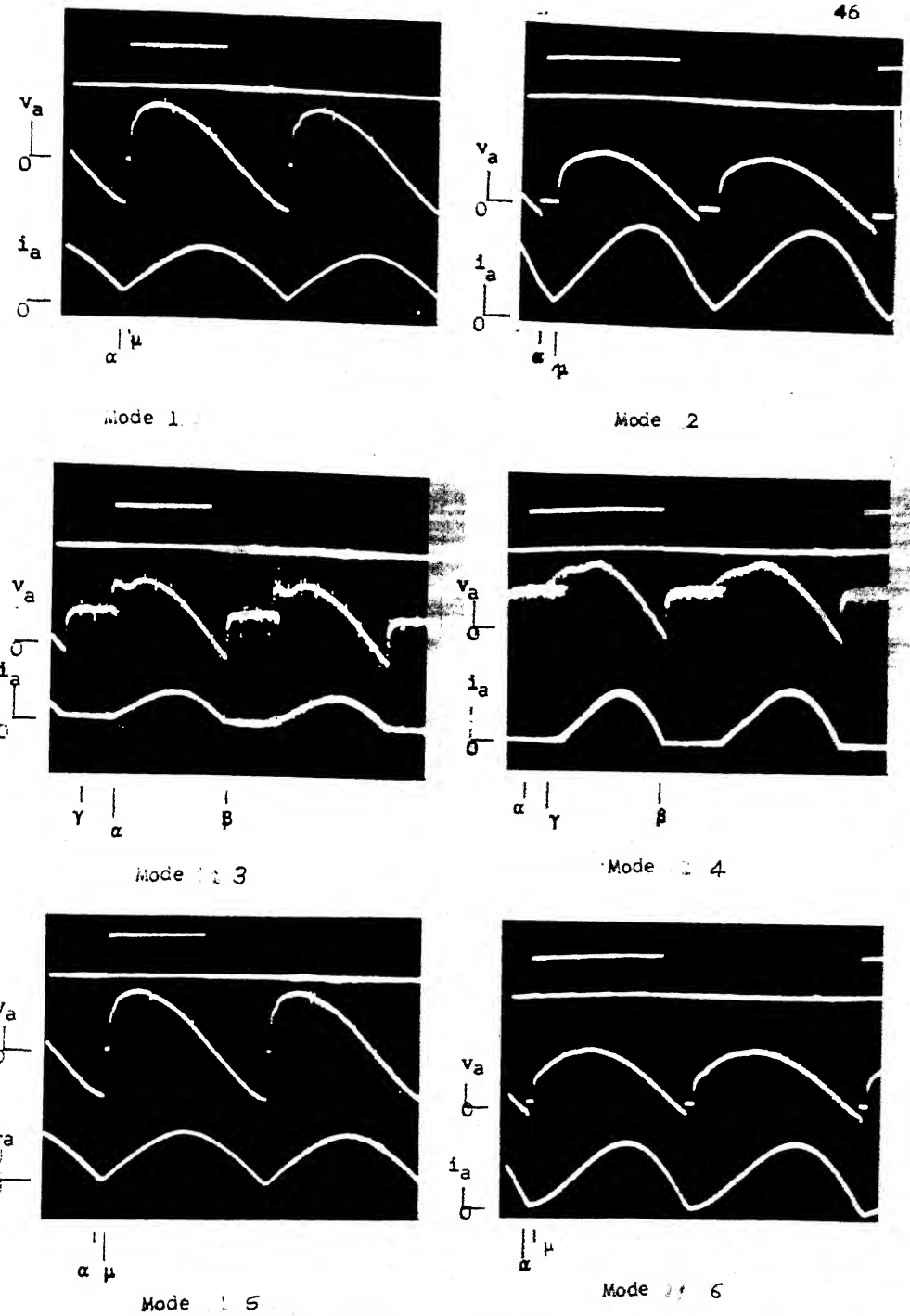

Fig. 4.6: Oscillograms

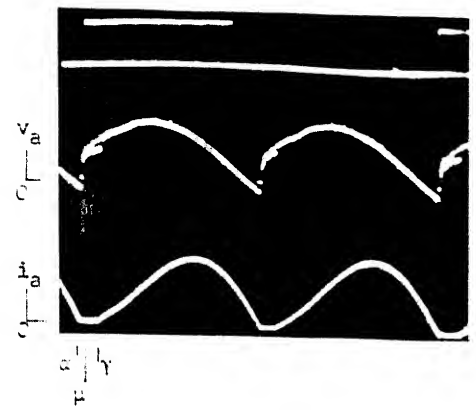

Mode 7

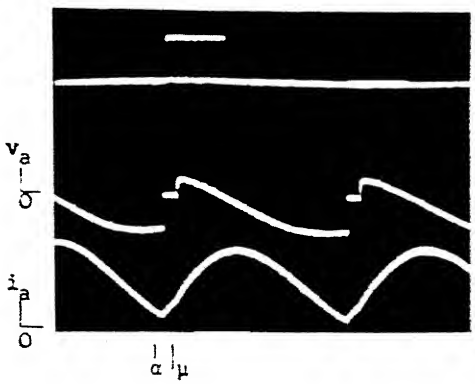

Mode 1 (inversion)

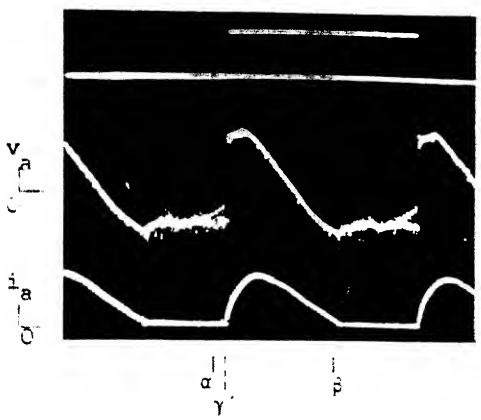

3
Mode (inversion)

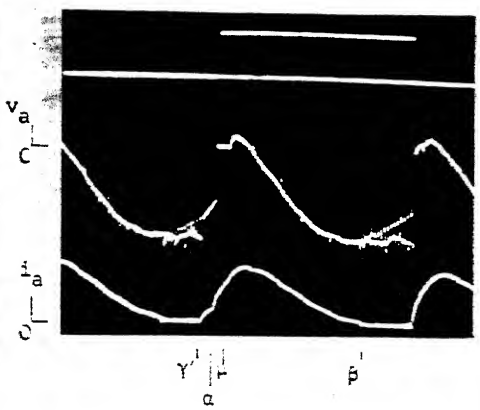

4
Mode (inversion)

Fig. 4.6: contd..

The experimental values of speed torque characteristics have been marked in these figures. This shows good correlation between the experimental and theoretical results.

From the speed-torque characteristics, it is obvious that as the source inductance increases the area of discontinuous current conduction decreases but speed regulation becomes poor. For a fixed firing angle, as the load increases speed drop becomes very large for higher values of source inductance.

Power factor, distortion factors and displacement factor have also been plotted for different values of source inductance at full load. These are shown in Fig. 4.11 and Fig. 4.12. The current distortion factor improves for increasing source inductance. Voltage distortion factor becomes poor because during commutation the voltage at both the ends of converter remains zero and commutation interval increases with source inductance and current. Displacement factor becomes poor due to higher degree of harmonics introduced and at large value of source inductance. Power factor is product of current distortion factor, voltage

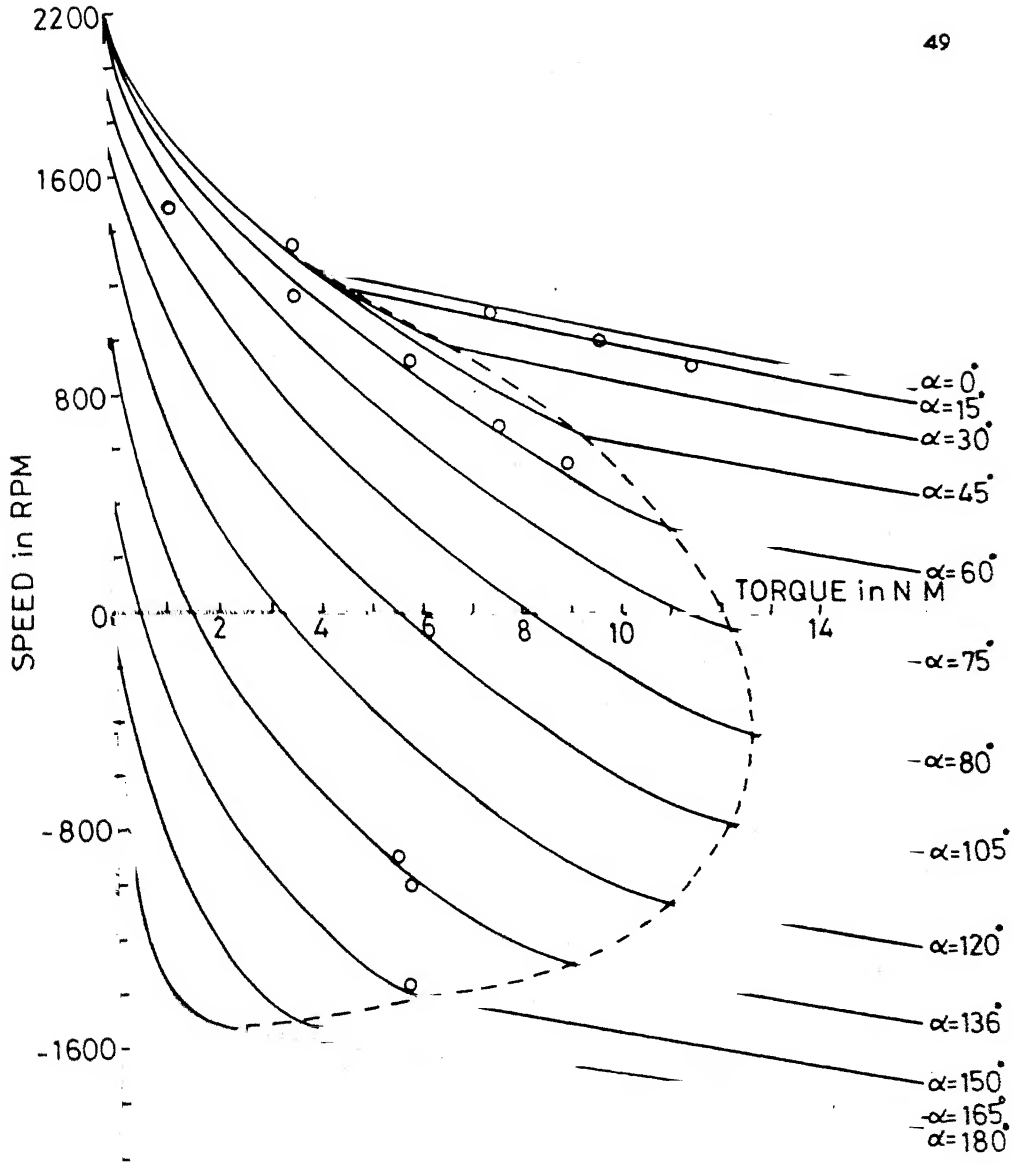

Fig. 4·7 L_S=0·0H

Speed-torque characteristics

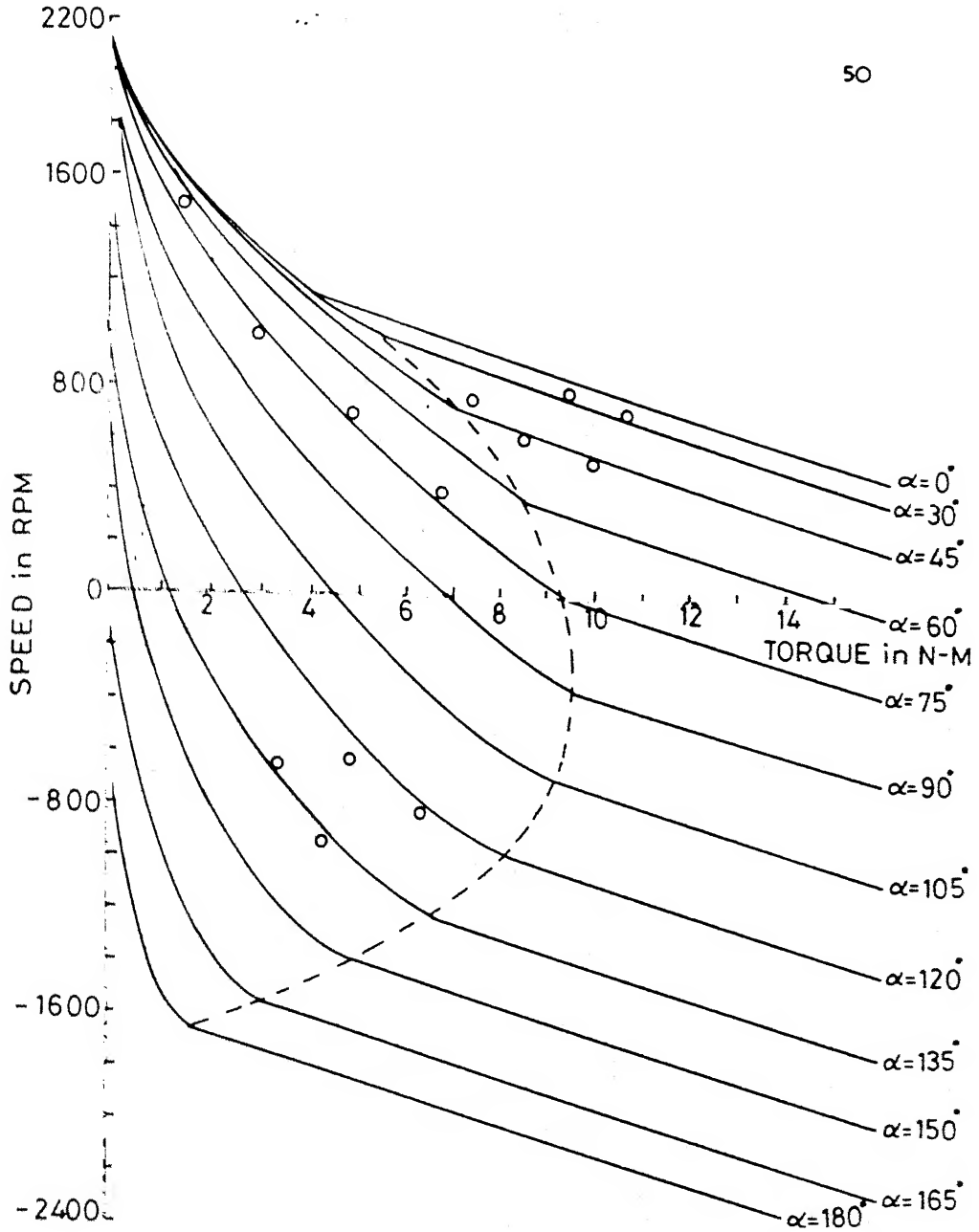

Fig. 4·8 L_S = ·009H

Speed-torque characteristics

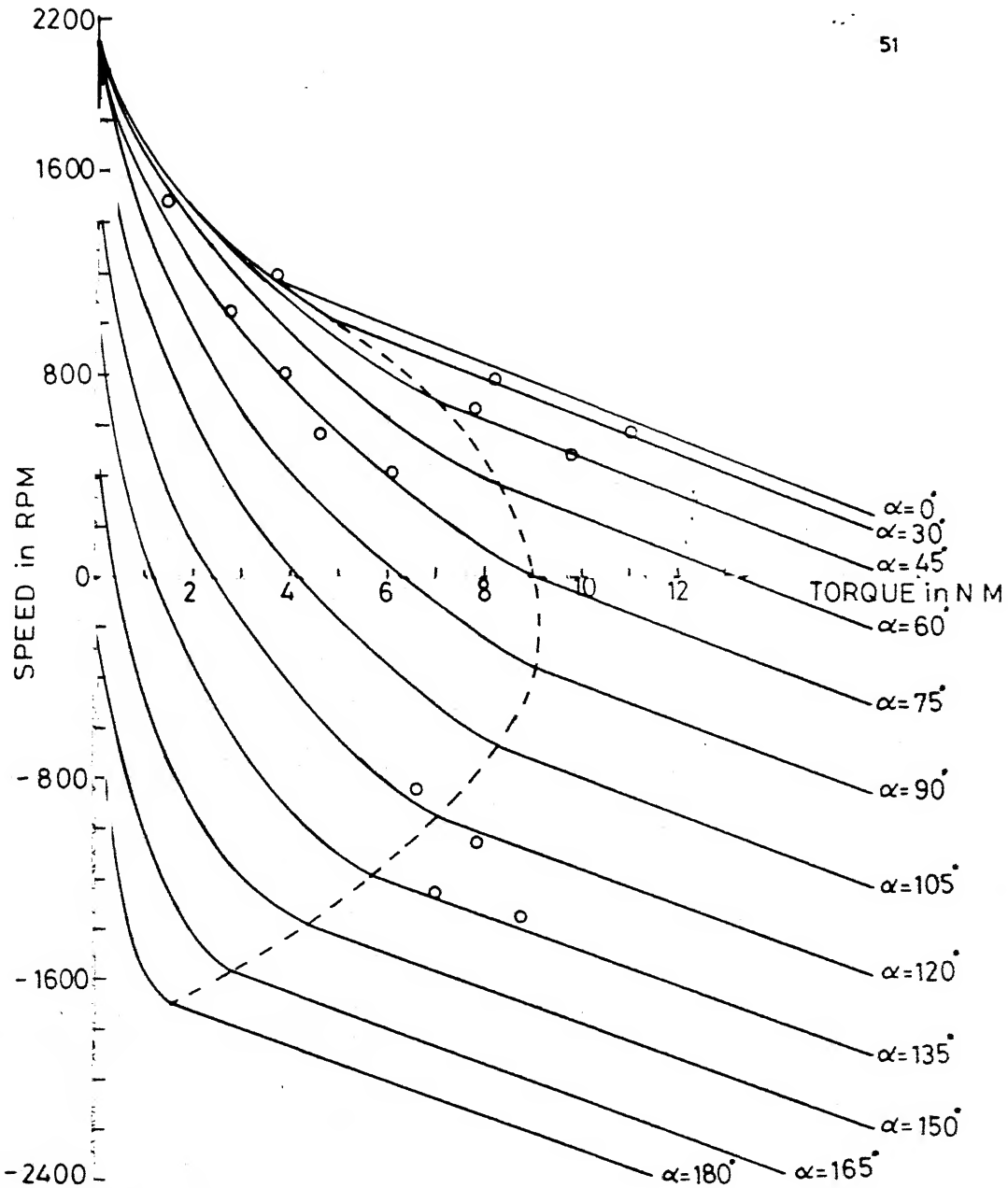

Fig. 4·9 L_S=·014H

Speed-torque characteristics

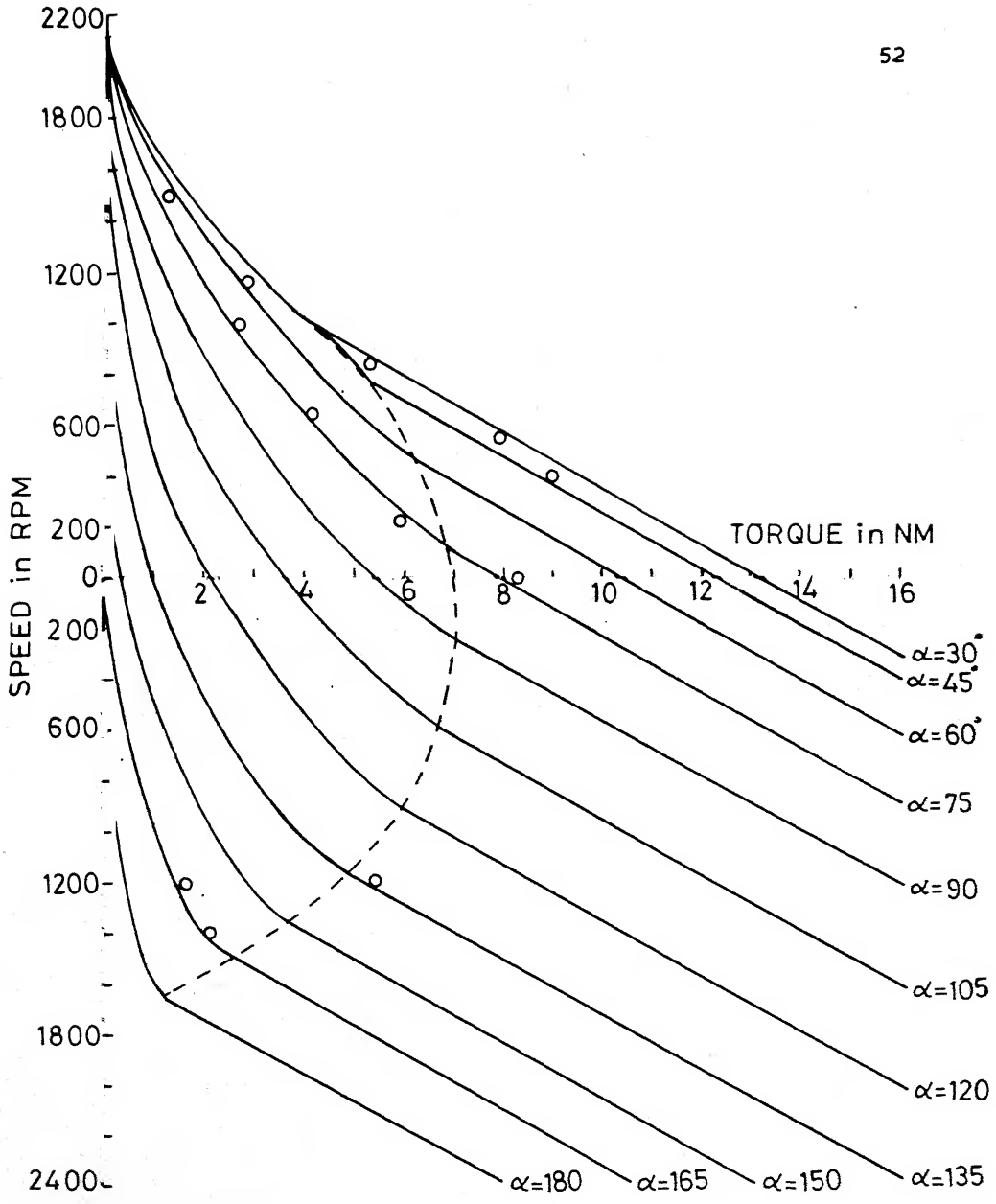

Fig.4·10 L_s=·024H
Speed-torque characteristics

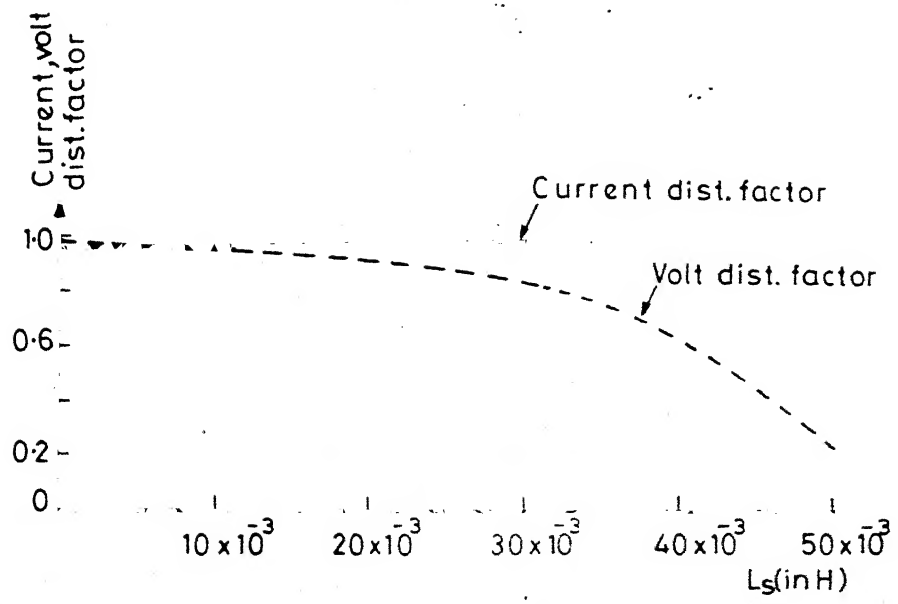

Fig. 4·11

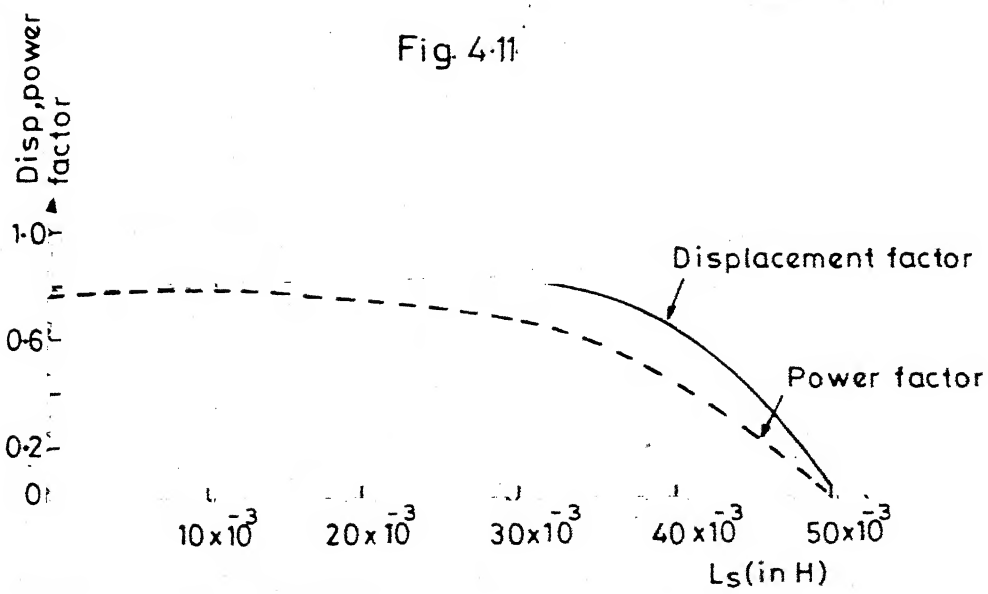

Fig. 4·12

distortion factors and displacement factor, hence the p.f. also reduces for increasing values of source inductance.

Therefore, the presence of source inductance causes the converter to operate at low power factor, thereby, drawing more reactive power. Losses are caused by ripples in armature current due to discontinuity. Also motor regulation is poor.

CHAPTER 5

CONCLUSION

In the present thesis, the performance of the single-phase fully controlled converter fed separately excited dc motor has been studied. Finite source inductance has been considered in this study. Firing of the pair of thyristors was maintained symmetrical. Different mode of operation have been described and experimentally observed. The oscillograms of some of the modes which occur during continuous or discontinuous armature current operation have been obtained. Regeneration has also been discussed along with rectification.

Speed-torque characteristics have been computed theoretically for different values of the source inductance. Experiment was also conducted to verify the theoretical deductions. Good correlation was found between the two. These characteristics show that the area of discontinuous operation is reduced when converter draws power from ac supply with finite source inductance. Motor speed regulation becomes poor. The ripples introduced due to discontinuous conduction contributes more copper losses. The performance of the drive becomes poor.

Current distortion factor improves but voltage distortion factor and displacement factor reduces with increasing load and source inductance. More harmonics are introduced and power factor becomes poor.

Therefore, the finite internal impedance present in ac supply introduces the finite delay called commutation interval during transfer of current from outgoing to incoming pair of thyristors. This gives rise to new modes of operation in rectification and regeneration operation. The presence of source inductance deteriorates the drive performance and causes the system to operate at reduced power factor.

REFERENCES

1. S.B. Dewan and A. Straughan, 'Power Semiconductor Circuits', A Willey Interscience Publication, New York, 1975.

2. Davis Fenney, 'The Power Thyristor and its Application', McGraw-Hill Book Company (UK), Ltd. 1980.

3. P.C. Sen, 'Thyristor DC Drives', A Willey-Interscience Publication, 1981.

4. Robinson C.E. 'Redesign of dc motors for Application with Thyristor Power Supplies', IEE Trans. 1968 IGA-4, pp. 508-514.

5. P. Mehta and S. Mukhapadhyay, 'Modes of Operation of Converter Controlled dc Drives', Proceedings of IEE, vol. 121, No. 3, March, 1974, p. 179.

6. Rechardson J., 'New Static Controller for dc Machines', Proceedings IEEE 1972, 119(11), pp. 1582-1585.

7. V. Subbiah and S. Palanichamy, 'Mode Identification and Minimum Inductance Estimation for Fully Controlled Thyristor Converters', IEEE Trans. on IECI, vol. 26, Feb. 1979, pp. 48.

8. G. Moltgan, 'Line Commutated Thyristor Converters', Siemens Asctiengesellschaft, Pitman Publishing, 1972.

9. P.B. Anjanayulu, P.S. Bhat, S.S. Prabhu, G.K. Dubey and R. Ghosh, 'Calculation of Filter Inductance for Converter Controlled dc Separately Excited Motor', Journal of the Institution of Engineers (I), vol. 65, Pt. EL4, Feb. 1985, pp. 105.

10. B.K. Patel and S.R. Doradla, 'Operating diagram and minimum Inductance Estimation for Fully Controlled Converter with Half Controlled Characteristics', Journal of the Institution of Engineers (I), vol. 62, Pt. EL-4, Feb. 1982, pp. 150.

11. P.S. Bhat and G.K. Dubey, 'Performance and Analysis of dc Motor Fed by Single-phase Converter with Controlled Flywheeling', Journal of the Institution of Engineers (I), vol. 65, Pt. EL-5, April, 1985.

12. H.M. El-Bolock and W. Shepherd, 'The Effect of Source Impedance on the Performance of Thyristor-Controlled Separately Excited dc Motor with Single-phase Supply', IEEE Trans. on Industrial Electronics, vol. IE-30, No. 4, Nov. 1983, pp. 357.

APPENDIX

DC motor specifications:

Output power	: 2.2 KW
Armature voltage	: 220V
Shunt field excitation	: 220V
Current rating	: 11.6A
Rated speed	: 1500 rpm
Armature resistance	: 2.0 Ohms
Armature inductance	: 32 mH
Back emf constant	: 0.8595 volt/rad.per sec.
Torque constant	: 0.8595 volt/rad. per sec.

Inductance measured at the mains : 1.0 mH

Values of inductances inserted in the ac side of the converter : 9.0 mH

14 mH

24 mH

```
C=================================================================
C       EVALUATION OF PERFORMANCE CHARACTERISTCS OF SINGLE-PHASE
C       CONVERTER FED SEPARATELY EXCITED DC MOTOR
C=================================================================
C       I1=ARMATURE INSTANTANEOUS CURRENT;;I2=SOURCE INSTANTANEOUS
C       CURRENT;;VA=INSTANTANEOUS ARMATURE VOLTAGE;;VS=INSTANTANEOUS
C       CNVERTER I/P VOLT.;;IS=OVER ALL RMS CURRENT;;IS1=FUNDAMENTAL
C       RMS CURRENT;;VSS=OVER ALL RMS VOLT.;;VS1=FUNDAMENTAL RMS VOLT.
C       IDISTF=CURRENT DISTORTION FACTOR;;VDISTF=VOLT.DISTORTION FACTOR
C       ISPHI=FUNDAMENTAL CURRENT PHASE ANGLE;;VSPHI=FUNDAMETAL VOLT.
C       PHASE ANGLE;;IAV=AVEARMATURE CURRENT;;TAV=AVERAGE TORQE
C       M=BEMF CONSTANT;;K=TORQE CONSTANT;;BETA=EXTINCTION ANGLE
C       GAMA=ANGLE AT WHICH BEMF EQUALS INSTANTANEOUS AC VOLT.
C       M1=MODE;;MU=OVERLAP ANGLE
C=================================================================
        DIMENSION N2(800),I(800),VA(800),VS(800)
        REAL I1,I2,I3,I,L,LS,K,M,MU,IAV,IS,ISPHI,IS1,IDISTF
        COMPLEX Z1
        INTEGER Z,M1
        READ(20,*) ALPHA,LS,RPM,M,K,L,R,R1
        PI=3.14159
        IS=0.0;VSS=0.0;AVS1=0.0;BVS1=0.0;AIS1=0.0;BIS1=0.0
        H=PI*0.5/180;H1=H/0.5
        ALPHA=ALPHA*H1
        X=PI+ALPHA
        BEMF=M*RPM
        EM=140.0*SQRT(2.0)
        GAMA=ASIN(BEMF/EM)
        IF(BEMF.LT.0.0) GAMA=PI+GAMA
        Z=0;I1=.00001
        W=314.159;WT=ALPHA
        IF(GAMA.GT.ALPHA) WT=GAMA
C-----------------------------------------------------------------
C       MODE IDENTIFICATION
C-----------------------------------------------------------------
2       CALL RUNG(R,R1,EM,WT,H,BEMF,L,LS,I1,V,V1)
        IF((BEMF.LT.0.0).AND.(GAMA.LT.ALPHA)) GO TO 3
3       IF(WT.GE.ALPHA) GO TO 5
        IF(I1) 61,61,4
4       WT=WT+H;IF(WT-X) 2,2,5
5       DO 16 N1=1,10
        WT=ALPHA
        DO 10 N=1,500
        IF(LS.LE.0.0001) GO TO 12

        IF(N.EQ.1) I2=-I1
        CALL RUNG1(EM,I2,LS,R,R1,BEMF,WT,H,L,I1)
        IF((I1.LT.0.0001).AND.(WT.GT.GAMA)) GO TO 91
8       WT=WT+H;IF(I1) 12,12,9
9       MU=WT;IF(I1-I2) 12,12,10
10      CONTINUE
12      DO 14 N=1,500
        CALL RUNG(R,R1,EM,WT,H,BEMF,L,LS,I1,V,V1)
        IF((I1.LT.0.0001).AND.(ALPHA.LT.GAMA)) GO TO 111
        IF((BEMF.LT.0.0).AND.(I1.LE.0.0)) GO TO 261
        IF(I1) 16,16,15
15      WT=WT+H;IF(WT-X) 14,14,16
14      CONTINUE
16      CONTINUE
        WT=ALPHA
        DO 24 N=1,500
        IF(LS.LE.0.0001) GO TO 28
        IF(N.EQ.1) I2=-I1
        CALL RUNG1(EM,I2,LS,R,R1,BEMF,WT,H,L,I1)
18      WT=WT+H;IF(I1) 20,20,22
20      MU=WT;IF(MU-GAMA) 91,91,71
22      IF(I1-I2) 28,28,24
24      CONTINUE
28      DO 34 N=1,500
        CALL RUNG(R,R1,EM,WT,H,BEMF,L,LS,I1,V,V1)
        WT=WT+H
32      IF(WT-X) 34,34,30
34      CONTINUE
C-----------------------------------------------------------------
C       FOLLOWING COMPUTATIONS ARE FOR MODE-1
```

```
      M1=11;IF(GAMA.GT.ALPHA) M1=12
      DO 60 N1=1,2
1     SUM=0;Z=0;WT=ALPHA;V1=EM*SIN(WT)
0     DO 45 N=1,500
      Z=Z+1;I(Z)=I1;VA(Z)=0;VS(Z)=0;W2(Z)=WT;SUM=SUM+H*I1;WT=WT+H
      IF(LS.LE.0.0001) GO TO 50

      IF(N.EQ.1) I2=-I1
      CALL RUNG1(EM,I2,LS,R,R1,BEMF,WT,H,L,I1)
      I3=I2;IF(N1.EQ.2) WT=WT+PI;IF(N1.EQ.2)I3=-I2
      CALL FS(H,IS,VSS,AIS1,BIS1,AVS1,BVS1,WT,I3,V1,VM,V)
      V1=0;IF(N1.EQ.2) WT=WT-PI
2     IF(LS.EQ.0) GOTO 45
      IF(I1-I2) 50,50,45
5     CONTINUE
0     DO 55 N=1,500
      Z=Z+1;I(Z)=I1;VA(Z)=V;VS(Z)=V1;W2(Z)=WT;SUM=SUM+H*I1;WT=WT+H
      CALL RUNG(R,R1,EM,WT,H,BEMF,L,LS,I1,V,V1)
      V2=(EM*SIN(WT)-(R+R1)*I1-BEMF)/(L+LS)
      I3=I1;IF(N1.EQ.2)WT=WT+PI;IF(N1.EQ.2)I3=-I1
      IF(N1.EQ.2) V2=-V2;V1=EM*SIN(WT)-R1*I3-LS*V2
      CALL FS(H,IS,VSS,AIS1,BIS1,AVS1,BVS1,WT,I3,V1,VM,V)
      IF(N1.EQ.2) WT=WT-PI
      IF(WT-X) 55,55,60
5     CONTINUE
0     CONTINUE
      BETA=PI
      IAV=SUM/PI
      TAV=K*IAV
      GO TO 150
C-----------------------------------------------------------------
C       FOLLOWING COMPUTATIONS ARE FOR MODE-2
C-----------------------------------------------------------------
1     M1=21;IF(GAMA.GT.ALPHA) M1=22
      DO 67 N1=1,2
      Z=0;I1=0.00001;V=BEMF;WT=ALPHA;SUM=0
      IF(ALPHA.LT.GAMA) WT=GAMA;V1=EM*SIN(WT)
      DO 65 N=1,500
      Z=Z+1;I(Z)=I1;W2(Z)=WT;VA(Z)=V;VS(Z)=V1;SUM=SUM+I1*H;WT=WT+H
      CALL RUNG(R,R1,EM,WT,H,BEMF,L,LS,I1,V,V1)
      V2=(EM*SIN(WT)-(R+R1)*I1-BEMF)/(L+LS)
      I3=I1;IF(N1.EQ.2) I3=-I1;IF(N1.EQ.2)WT=WT+PI
      IF(N1.EQ.2) V2=-V2;V1=EM*SIN(WT)-R1*I3-LS*V2
      CALL FS(H,IS,VSS,AIS1,BIS1,AVS1,BVS1,WT,I3,V1,VM,V)
      IF(N1.EQ.2)WT=WT-PI
      IF(I1.LE..001) GO TO 70
5     CONTINUE
0     MU=0
      BETA=WT-ALPHA;IF(GAMA.GT.ALPHA) BETA=WT-GAMA
      DO 66 N=1,500
      Z=Z+1;I(Z)=0.0001;VA(Z)=BEMF;VS(Z)=V1;W2(Z)=WT
      I3=0;V1=EM*SIN(WT)
      CALL FS(H,IS,VSS,AIS1,BIS1,AVS1,BVS1,WT,I3,V1,VM,V)
      WT=WT+H
      IF((M1.EQ.21).AND.(WT.GT.K)) GO TO 67
      IF((M1.EQ.22).AND.(WT.GT.(PI+GAMA))) GO TO 67
6     CONTINUE
7     CONTINUE
      IAV=SUM/PI
      TAV=K*IAV
      GO TO 150
C-----------------------------------------------------------------
C       FOLLOWING CMPUTATIONS ARE FOR MODE-3 OF INVERSION
C-----------------------------------------------------------------
261   M1=3;DO 295 N1=1,2
      WT=GAMA;V=BEMF;SUM=0;Z=0;I1=0.00001;V1=EM*SIN(WT)
      DO 265 N=1,500
      Z=Z+1;I(Z)=I1;W2(Z)=WT;VA(Z)=V;VS(Z)=V1;SUM=SUM+I1*H;WT=WT+H;
      EM=-EM;CALL RUNG(R,R1,EM,WT,H,BEMF,L,LS,I1,V,V1)
      V2=(EM*SIN(WT)-(R+R1)*I1-BEMF)/(L+LS);I3=I1
      IF(N1.EQ.2) I3=-I1;IF(N1.EQ.2) WT=WT+PI
      IF(N1.EQ.2) V2=-V2;V1=EM*SIN(WT)-R1*I3-LS*V2
      CALL FS(H,IS,VSS,AIS1,BIS1,AVS1,BVS1,WT,I3,V1,VM,V)
      IF(N1.EQ.2) WT=WT-PI;IF(WT.GE.ALPHA) GO TO 266
```

```
265       CONTINUE
266       EM=-EM
          IF(LS.LE..0001) GO TO 275
          DO 270 N=1,500
          IF(N.EQ.1) I2=-I1
          Z=Z+1;I(Z)=I1;W2(Z)=WT;VA(Z)=0;VS(Z)=0;SUM=SUM+I1*H;WT=WT+H
          CALL RUNG1(EM,I2,LS,R,R1,BEMF,WT,H,L,I1)
          I3=I2;IF(N1.EQ.2)WT=WT+PI;IF(N1.EQ.2)I3=-I2
          V1=0.0;CALL FS(H,IS,VSS,AIS1,BIS1,AVS1,BVS1,WT,I3,V1,VM,V)
          IF(N1.EQ.2)WT=WT-PI
          IF(I1+I2) 275,275,270
270       CONTINUE
275       DO 280 N=1,500
          Z=Z+1;I(Z)=I1;W2(Z)=WT;VA(Z)=V;VS(Z)=V1;SUM=SUM+I1*H;WT=WT+H
          CALL RUNG(R,R1,EM,WT,H,BEMF,L,LS,I1,V,V1)
          V2=(EM*SIN(WT)-(R+R1)*I1-BEMF)/(L+LS);I3=I1
          IF(N1.EQ.2) I3=-I1;IF(N1.EQ.2) WT=WT+PI
          IF(N1.EQ.2) V2=-V2;V1=EM*SIN(WT)-R1*I3-LS*V2
          CALL FS(H,IS,VSS,AIS1,BIS1,AVS1,BVS1,WT,I3,V1,VM,V)
          IF(N1.EQ.2) WT=WT-PI;IF(I1) 285,285,280
280       CONTINUE
285       MU=0;BETA=WT-GAMA
          DO 290 N=1,500
          Z=Z+1;I(Z)=I1;W2(Z)=WT;VA(Z)=V;VS(Z)=V1;WT=WT+H
          I1=0;I3=0;V1=EM*SIN(WT)
          CALL FS(H,IS,VSS,AIS1,BIS1,AVS1,BVS1,WT,I3,V1,VM,V)
          IF(WT.GE.(GAMA+PI)) GO TO 295
290       CONTINUE
295       CONTINUE
          IAV=SUM/PI;TAV=K*IAV
          GO TO 150
C---------------------------------------------------------------------
C         FOLLOWING  COMPUTATIONS ARE FOR MODE-3
C---------------------------------------------------------------------
71        M1=31;IF(GAMA.GT.ALPHAD) M1=32
          DO 90 N1=1,2
          I1=0.00001;Z=0;SUM=0;WT=MU;V=BEMF;V1=EM*SIN(WT)
          DO 75 N=1,500
          T1=I1;IF(N1.EQ.2)I1=-T1
          Z=Z+1;I(Z)=I1;W2(Z)=WT;VA(Z)=V;VS(Z)=V1;SUM=SUM+I1*H;WT=WT+H
          CALL RUNG(R,R1,EM,WT,H,BEMF,L,LS,I1,V,V1)
          V2=(EM*SIN(WT)-(R+R1)*I1-BEMF)/(L+LS)
          I3=I1;IF(N1.EQ.2) WT=WT+PI;IF(N1.EQ.2) I3=-I1
          IF(N1.EQ.2) V2=-V2;V1=EM*SIN(WT)-R1*I3-LS*V2
          CALL FS(H,IS,VSS,AIS1,BIS1,AVS1,BVS1,WT,I3,V1,VM,V)
          IF(N1.EQ.2)WT=WT-PI
          IF(WT-X) 75,75,80
75        CONTINUE
80        DO 85 N=1,500
          IF(LS.LE.0.0001) GO TO 90
          IF(N.EQ.1) I2=I1
          Z=Z+1;I(Z)=I1;W2(Z)=WT;VA(Z)=0;VS(Z)=0;SUM=SUM+H*I1;WT=WT+H
          CALL RUNG1(EM,I2,LS,R,R1,BEMF,WT,H,L,I1)
          I3=I2;IF(N1.EQ.2) WT=WT+PI;IF(N1.EQ.2) I3=-I2
          V1=0.0;CALL FS(H,IS,VSS,AIS1,BIS1,AVS1,BVS1,WT,I3,V1,VM,V)
          IF(N1.EQ.2)WT=WT-PI
82        IF(I1.LE..001) GO TO 90
85        CONTINUE
90        CONTINUE
          MU=WT-PI
          IAV=SUM/PI
          TAV=K*IAV
          BETA=WT-MU
          GO TO 150
C---------------------------------------------------------------------
C         FOLLOWING COMPUTATIONS ARE FOR MODE-4
C---------------------------------------------------------------------
91        M1=4
          DO 107 N1=1,2
          Z=0;I1=0.00001;SUM=0;WT=GAMA;V=BEMF;V1=EM*SIN(WT)
          DO 95 N=1,500
          T1=I1;IF(N1.EQ.2) T1=-T1
          Z=Z+1;I(Z)=I1;W2(Z)=WT;VA(Z)=V;VS(Z)=V1;SUM=SUM+I1*H;WT=WT+H
          CALL RUNG(R,R1,EM,WT,H,BEMF,L,LS,I1,V,V1)
          V2=(EM*SIN(WT)-(R+R1)*I1-BEMF)/(L+LS)
```

```
      I3=I1;IF(N1.EQ.2)WT=WT+PI;IF(N1.EQ.2) I3=-I1
      IF(N1.EQ.2) V2=-V2;V1=EM*SIN(WT)-R1*I3-LS*V2
      CALL FS(H,IS,VSS,AIS1,BIS1,AVS1,BVS1,WT,I3,V1,VM,V)
      IF(N1.EQ.2) WT=WT-PI
      IF(WT-X) 95,95,100
95    CONTINUE
100   DO 105 N=1,500
      IF(LS.LE.0.0001) GO TO 110
      IF(N.EQ.1) I2=I1
      Z=Z+1;I(Z)=I1;W2(Z)=WT;VA(Z)=0;VS(Z)=0;SUM=SUM+I1*H;WT=WT+H
      CALL RUNG1(EM,I2,LS,R,R1,BEMF,WT,H,L,I1)
      I3=I2;IF(N1.EQ.2) WT=WT+PI;IF(N1.EQ.2) I3=-I2
      V1=0.0;CALL FS(H,IS,VSS,AIS1,BIS1,AVS1,BVS1,WT,I3,V1,VM,V)
      IF(N1.EQ.2) WT=WT-PI
99    IF(I1.LE..001) GO TO 110
105   CONTINUE
110   MU=WT-PI
      BETA=WT-GAMA
      DO 106 N=1,500
      Z=Z+1;I(Z)=I1;W2(Z)=WT;VA(Z)=BEMF;VS(Z)=0;WT=WT+H
      IF(N1.EQ.2) WT=WT+PI;I3=0;I1=0;V1=EM*SIN(WT)
      CALL FS(H,IS,VSS,AIS1,BIS1,AVS1,BVS1,WT,I3,V1,VM,V)
      IF(N1.EQ.2) WT=WT-PI
      IF(WT.GE.(GAMA+PI)) GO TO 107
106   CONTINUE
107   CONTINUE
      IAV=SUM/PI
      TAV=IAV*K
      GO TO 150
C-----------------------------------------------------------------
C     FOLLOWING COMPUTATION ARE FOR MODE-5
C-----------------------------------------------------------------
111   M1=5
      DO 147 N1=1,2
      I1=.000010;Z=0;SUM=0;WT=GAMA;V=BEMF;V1=EM*SIN(WT)
      DO 115 N=1,500
      T1=T1;IF(N1.EQ.2) T1=-T1
      Z=Z+1;I(Z)=I1;W2(Z)=WT;SUM=SUM+I1*H;VA(Z)=V;VS(Z)=V1;WT=WT+H
      CALL RUNG(R,R1,EM,WT,H,BEMF,L,LS,I1,V,V1)
      V2=(EM*SIN(WT)-(R+R1)*I1-BEMF)/(L+LS)
      I3=I1;IF(N1.EQ.2)WT=WT+PI;IF(N1.EQ.2) I3=-I1
      IF(N1.EQ.2)V2=-V2;V1=EM*SIN(WT)-R1*I3-LS*V2
      CALL FS(H,IS,VSS,AIS1,BIS1,AS1,BVS1,WT,I3,V1,VM,V)
      IF(N1.EQ.2) WT=WT-PI
      IF(WT-X) 115,115,120
115   CONTINUE
120   DO 125 N=1,500
      IF(LS.LE.0.0001) GO TO 130
      IF(N.EQ.1) I2=I1
      Z=Z+1;I(Z)=I1;W2(Z)=WT;VA(Z)=0;VS(Z)=0;SUM=SUM+H*I1;WT=WT+H
      CALL RUNG1(EM,I2,LS,R,R1,BEMF,WT,H,L,I1)
      I3=I2;IF(N1.EQ.2) WT=WT+PI;IF(N1.EQ.2) I3=-I2
      V1=0;CALL FS(H,IS,VSS,AIS1,BIS1,AVS1,BVS1,WT,I3,V1,VM,V)
      IF(N1.EQ.2) WT=WT-PI
      IF(I1+I2)130,130,125
122   IF(I1) 130,130,125
125   CONTINUE
130   MU=WT-PI
      DO 140 N=1,500
      T1=I1;IF(N1.EQ.2) T1=-T1
      Z=Z+1;I(Z)=I1;W2(Z)=WT;VA(Z)=V;VS(Z)=V1;SUM=SUM+H*I1;WT=WT+H
      CALL RUNG(R,R1,EM,WT,H,BEMF,L,LS,I1,V,V1)
      V2=(EM*SIN(WT)-(R+R1)*I1-BEMF)/(L+LS)
      I3=I1;IF(N1.EQ.2) WT=WT+PI;IF(N1.EQ.2) I3=-I1
      IF(N1.EQ.2)V2=-V2;V1=EM*SIN(WT)-R1*I3-LS*V2
      CALL FS(H,IS,VSS,AIS1,BIS1,AVS1,BVS1,WT,I3,V1,VM,V)
      IF(N1.EQ.2) WT=WT-PI
      IF(I1.LE..001) GO TO 145
140   CONTINUE
145   BETA=WT-GAMA
      DO 146 N=1,500
      Z=Z+1;I(Z)=I1;W2(Z)=WT;VA(Z)=V;VS(Z)=V1;WT=WT+H
      IF(N1.EQ.2) WT=WT+PI;I3=0;I1=0;V1=EM*SIN(WT)
      CALL FS(H,IS,VSS,AIS1,BIS1,AVS1,BVS1,WT,I3,V1,VM,V)
      IF(N1.EQ.2) WT=WT-PI
```

```
      IF(WT.GE.(GAMA+PI)) GO TO 147
146   CONTINUE
147   CONTINUE
      IAV=SUM/PI
      TAV=K*IAV
150   ALPHA=ALPHA/H1;BETA=BETA/H1;GAMA=GAMA/H1;MU=MU/H1
      BIS1=BIS1/PI
      AIS1=AIS1/PI;AVS1=AVS1/PI;BVS1=BVS1/PI
      IS=IS/(2*PI);IS=SQRT(IS);VSS=VSS/(2*PI);VSS=SQRT(VSS)
      IS1=(AIS1**2+BIS1**2)/2;VS1=(AVS1**2+BVS1**2)/2
      IS1=SQRT(IS1);VS1=SQRT(VS1);VSPHI=ATAN(AVS1/BVS1)
      ISPHI=ATAN(AIS1/BIS1);VDISTF=VS1/VSS;IDISTF=IS1/IS
      DISP=COS(ISPHI-VSPHI);PF=VDISTF*IDISTF*DISP;VM=VM/PI
      WRITE(21,152) ALPHA,BETA,GAMA,IAV,TAV,MU,BEMF,LS,RPM,M1
      WRITE(21,152) PF,VDISTF,IDISTF,DISP,VM,IS1,VS1,VSS,IS,M1
152   FORMAT(4X,9F13.3,I10)
      L1=1
      DO 171 N=1,Z
      L2=L1+1;L3=L2+1;L4=L3+1
      WRITE(21,170) W2(L1),I(L1),VA(L1),W2(L2),I(L2),VA(L2),W2(L3)
     1,I(L3),VA(L3),W2(L4),I(L4),VA(L4)
      IF(L4.GE.Z) GO TO 1000
      L1=L4+1
171   CONTINUE
170   FORMAT(4X,12F10.2)
151   IF(IAV.GE.12.0) GO TO 1000;RPM=RPM-100;GO TO 1
192   IF(ALPHA-180) 190,100),1000
190   ALPHA=ALPHA+15;RPM=1500;GO TO 1
1000  STOP
      END
      SUBROUTINE RUNG(R,R1,EM,WT,H,BEMF,L,LS,I1,V,V1)
      REAL LS,I1,L
      T1=I1
      DEL1=H*(EM*SIN(WT)-BEMF-(R+R1)*I1)/((L+LS)*314.159)
      DEL2=H*(EM*SIN(WT+H/2)-BEMF-(R+R1)*(I1+DEL1/2))/((L+LS)*314.1
      DEL3=H*(EM*SIN(WT+H/2)-BEMF-(R+R1)*(I1+DEL2/2))/((L+LS)*314.1
      DEL4=H*(EM*SIN(WT+H)-BEMF-(R+R1)*(I1+DEL3))/((L+LS)*314.159)
      I1=I1+(DEL1+2*DEL2+2*DEL3+DEL4)/6
      V=2.5*T1+BEMF+L*(I1-T1)*314.159/H
      RETURN
      END
      SUBROUTINE RUNG1(EM,I2,LS,R,R1,BEMF,WT,H,L,I1)
      REAL I1,L,LS,I2
      DEL1=H*(-BEMF-R*I1)/(L*314.159)
      DEL2=H*(-BEMF-R*(I1+DEL1/2))/(L*314.159)
      DEL3=H*(-BEMF-R*(I1+DEL2/2))/(L*314.159)
      DEL4=H*(-BEMF-R*(I1+DEL3))/(L*314.159)
      I1=I1+(DEL1+2*DEL2+2*DEL3+DEL4)/6
      DEL1=H*(EM*SIN(WT)-R1*I2)/(LS*314.159)
      DEL2=H*(EM*SIN(WT+H/2)-R1*(I2+DEL1/2))/(LS*314.159)
      DEL3=H*(EM*SIN(WT+H/2)-R1*(I2+DEL2/2))/(LS*314.159)
      DEL4=H*(EM*SIN(WT+H)-R1*(I2+DEL3))/(LS*314.159)
      I2=I2+(DEL1+2*DEL2+2*DEL3+DEL4)/6
      RETURN
      END
      SUBROUTINE FS(H,IS,VSS,AIS1,BIS1,AVS1,BVS1,WT,I3,V1,VM,V)
      REAL I3,IS
      IS=IS+(I3**2)*H;VSS=VSS+(V1*V1)*H;AIS1=AIS1+H*I3*COS(WT)
      BIS1=BIS1+H*I3*SIN(WT);AVS1=AVS1+H*V1*COS(WT)
      BVS1=BVS1+H*V1*SIN(WT);VM=VM+V*H
      RETURN;END
```

EE-1986-M-CHA-EFF